The Volatility-of-Volatility Term Structure

Nicole Branger* Hendrik Hülsbusch* Alexander Kraftschik*

This version: October 19, 2017

Abstract

This paper investigates the volatility-of-volatility (VVIX) term structure. The term structure is in nearly all cases downward sloping. We find that the slope of the VVIX ($\text{Slope}^{\text{VVIX}}$), defined as VVIX' second principal component, predicts excess returns of S&P500 and VIX straddles. Its informational content is incremental to the VIX term structure and to the variance risk premium. To analyze which type of risk is captured by $\text{Slope}^{\text{VVIX}}$, we develop an affine approximation for the VVIX based on a VIX option pricing model. We find that the contributions of continuous vol-of-vol and jump risk to the term structure vary systematically with the state of the economy. When the latest major crises hit, continuous vol-of-vol took the lion's share over all maturities. As its relative contribution is similarly high across all maturities at these times, our results suggest that investors expected a prolonged period of high uncertainty in volatility.

Keywords: Financial Crises, Option Returns, Term Structure, Volatility, Volatility-of-Volatility, VVIX

JEL: C13, G01, G12, G13, G17

* School of Business and Economics, Finance Center Muenster, University of Muenster, Universitätsstr. 14-16, 48143 Münster, Germany. E-mail: nicole.branger@wiwi.uni-muenster.de, hendrik.huelsbusch@wiwi.uni-muenster.de, alexander.kraftschik@wiwi.uni-muenster.de

We thank Torben G. Andersen, Thijs van der Heijden, Iman Honarvar, Roger Laeven, Franck Moraux, Marek Musiela, Yang-Ho Park, Oliver Rieger, Christian Schlag, Michael Semenischev, Viktor Todorov, Servaas van Bilsen, seminar participants at the Amsterdam School of Economics as well as participants at the Quantitative Methods in Finance (QMF) 2015 Conference, the 33rd French Finance Association Conference (AFFI 2016), the Financial Econometrics and Empirical Asset Pricing Conference in Lancaster 2016, the 20th Annual Conference of the Swiss Society for Financial Market Research (SGF 2017), the 24th Annual Meeting of the German Finance Association (DGF 2017) and participants of the SoFiE Financial Econometrics Summer School (2017) at the Kellogg School of Management for helpful comments and suggestions.

1 Introduction

Volatility is a key determinant for financial pricing models and expected returns. By the introduction of derivatives on the volatility index VIX, stock market uncertainty became a publicly tradable asset for all market participants.[1] The high liquidity of VIX options over a large range of strike prices makes it feasible to study volatility in more detail. This paper investigates the term structure of model-free implied volatility-of-volatility (VVIX), which captures the expected risk-neutral variation of the VIX. First, we document that the slope of the VVIX term structure, not its level, is a significant risk factor for index stock and volatility option returns. This risk factor coexists next to the slope of the VIX and the variance risk premium (VRP). Second, we find the slope of the VVIX to capture volatility-of-volatility (*vol-of-vol*) risk better than the level, because the latter is too sticky at the peak of market turmoil. Third, we analyze two possible drivers of the VVIX term structure: jumps and continuous vol-of-vol risk. A newly developed decomposition based on a full market model shows that both components contribute differently to the term structure, depending on market conditions. In calm times, the slope of the term structure is mainly driven by jump expectations, whereas continuous vol-of-vol expectations are the driving force in times of distress.

We start with an empirical analysis of the VVIX term structure, which we calculate from VIX option prices, ranging from September 2007 to August 2014. In over 95 percent of this sample, the VVIX term structure was downward sloping, meaning that, in risk neutral terms, market participants expected the vol-of-vol to decrease.[2]

[1] VIX futures where introduced by the CBOE in 2004, VIX options followed two years later. By now, the trading volume of VIX options makes up to more than 60% of the trading volume of standard and weekly S&P500 options.

[2] This behavior is opposite to the behavior of the VIX and VRP term structure. Ait-Sahalia, Karaman, and Mancini (2015) amongst others show that the term structure of the VIX and VRP is upward sloping.

To describe the informational content of the term structure, we look at the first and second principal component which we define as $Level^{VVIX}$ and $Slope^{VVIX}$, respectively. Our results show that the VVIX term structure carries different information compared to the VIX and the variance risk premium (VRP). For all maturities, the VVIX term structure is rather independent of the VIX term structure and the VRP. To examine whether the level and slope of the VVIX also represent distinct risk factors, we conduct predictive regressions for volatility products, which are mainly exposed to volatility and vol-of-vol risk. More specifically, we study the predictive power for daily returns of VIX and S&P500 straddles. Our predictive regressions show that $\text{Slope}^{\text{VVIX}}$ forecasts these straddle returns with a positive sign and that this predictive power is incremental to the VRP and to $\text{Slope}^{\text{VIX}}$. This means that investors demand a premium for changes of expected vol-of-vol even on the stock option level.

While $\text{Slope}^{\text{VVIX}}$ has predictive power, $\text{Level}^{\text{VVIX}}$ has none. We reason this finding by the level's behavior at times of high market volatility. After the VIX peaks, $\text{Level}^{\text{VVIX}}$ remains at high levels, which we refer to as stickiness. In contrast the slope decreases quickly. This drives the wedge between the predictive power of both variables.

To shed light on the drivers behind the term structure, we rely on a jump-diffusion model, where the variance of stock returns (V) is exposed to jumps with time-varying intensity and diffusive vol-of-vol (q) risk. To estimate the model's parameters we choose to calibrate directly to the VVIX term structure, which we derive from the underlying VIX option prices on a weekly frequency. Afterwards, we provide a new approximation method to express the VVIX^2 and its term structure as a linear function of higher moments of the model's state variables. This approximation is similar to the affine representation of the VIX^2 in affine models and allows us to understand the different risk factors embedded in the VVIX.

Consistent with the empirical analysis and the literature, our affine representation of the VVIX[2] shows that current diffusive stock market volatility has almost no impact on the VVIX. Overall the VVIX is mainly driven by expected continuous vol-of-vol risk, which accounts on average for more than 55% at the short-end of the VVIX term structure and for almost 40% at the long-end. Variance jump risk makes an average contribution of 29% at the short end and 26% at the long end of the term structure. As a third constituent we find a time-dependent component A^{VVIX}, which is basically a constant plus a residual term that arises due to non-linear interdependencies of V and q. It accounts for 10% at the short-end, and roughly 25% at the long-end of the VVIX term structure. In sum, these three factors make up 95% of the term structure. Their relative and absolute contribution vary systematically over time, depending on the state of the economy. We identify the instantaneous variance-of-variance to variance (q/V) ratio as a well-suited measure to describe the economy's state.

Empirically, as well as in our model, VVIX is approximately a linear function of q/V, where the impact of q/V decreases in maturity. In case of a very low q/V-ratio, the term structure of the VVIX is mainly driven by variance jump expectations and A^{VVIX}. When q/V increases, continuous vol-of-vol risk gains importance quickly and makes up the major part of the VVIX across all maturities. At market turmoil, i.e. in case of a high q/V-ratio, jump risk looses its impact on the slope of the term structure and turns into a level component. As also A^{VVIX} becomes negligible, continuous vol-of-vol remains as the driving force behind the slope. Looking at the time periods around the three VIX peaks of 2008, 2010 and 2011 confirms this finding. At these times, the decomposition shows that $\text{Slope}^{\text{VVIX}}$ captures a change in the risk-composition of volatility risks from jump to continuous vol-of-vol risk. This implies that as soon as a crisis hits, volatility uncertainty takes over from jump expectations in relative terms. Since diffusive vol-of-vol risk is furthermore almost equally important at the short- and long-end of the term structure at the peak of

the crises, we conclude that investors expected volatility to remain highly uncertain for a long time.

There are already numerous studies on the term structure of volatility risk.[3] Closest to our work is Johnson (2016). He concentrates on the VIX term structure and shows that its slope predicts returns of a wide class of volatility derivatives, such as VIX futures and S&P500 straddles. Our empirical investigation confirms his results and extends them to vol-of-vol. While the VVIX term structure has, to the best of our knowledge, not yet been investigated, the VVIX for 30 days of maturity ($\text{VVIX}^{30\text{D}}$) and its associated risk premium has been addressed by Huang and Shaliastovich (2014), Park (2015), Hollstein and Prokopczuk (2017) and Kaeck (2017). The work of Huang and Shaliastovich (2014) reveals that vol-of-vol measured by the VVIX is related to a negative risk premium since it significantly predicts delta hedged VIX option returns. While they show that the $\text{VVIX}^{30\text{D}}$ is highly independent from the $\text{VIX}^{30\text{D}}$, we document that this independence also holds for longer maturities. Park (2015) proposes a tail risk interpretation for the $\text{VVIX}^{30\text{D}}$, since it forecasts adjusted delta hedged option returns of VIX and S&P500 options. Comparing different model-free variance measures, he concludes that the predictive power stems from the continuously integrated vol-of-vol. Hollstein and Prokopczuk (2017) show that volatility-of-volatility risk is priced in the cross-section of stocks with a significant negative risk premium. The analysis of Kaeck (2017) shows that the variance-of-variance risk premium is distinct from the VRP and significantly

[3]See for example Amengual (2008), Ait-Sahalia, Karaman, and Mancini (2015) and Luo and Zhang (2012). The term structure of the VIX has been analyzed e.g. by Luo and Zhang (2012) who show that the term structure is upward sloping and that it has predictive power for future realized volatilities. Amengual (2008) studies and tests models for the term structure of the variance risk premium. He shows that the VIX term structure is upward sloping. Ait-Sahalia, Karaman, and Mancini (2015) document a mostly upward sloping term structure of the VRP and conduct a model based analysis of the premiums. Throughout our paper, we define the VRP in terms of $\mathbb{Q}-\mathbb{P}$. Thus, for consistency the results are stated here in terms of an on average positive VRP.

negative, even after adjusting for several risk factors. Our model-based treatment of the term structure allows for a more detailed exploration of its drivers. To do so, we exploit the prices of VIX options, underlying the VVIX term structure. In the domain of VIX derivative pricing, seminal works are Sepp (2008a,b), Mencia and Sentana (2013) and Bardgett, Gourier, and Leippold (2016) amongst others.[4] For our purposes, we rely on a stochastic vol-of-vol model and augment it with variance jumps. The subsequent methodology to approximate the VVIX in a linear fashion is novel to the literature and is also applicable to other model setups.[5]

The remainder of the paper is structured as follows. The subsequent chapter explains the concept of model-free risk-neutral expectations of realized volatilities, our data set and the construction of the VVIX term structure. In chapter 2 we conduct predictive regressions for daily straddle returns. In chapter 3 we introduce the model and derive and test our affine VVIX^2 approximation. Chapter 4 contains our results for the risk factors of the VVIX term structure. Chapter 5 concludes.

2 VIX Futures, the VVIX and its Term Structure

2.1 VIX, VIX Options and the VVIX

The volatility index VIX provides a model-free measure of market participants' risk-neutral expectation of market return volatility. It thereby provides a valuable indicator of market uncertainty and has drawn the attention of researchers, practitioners and private investors alike. For a maturity of $\tau = \frac{30}{365}$, the Chicago Board

[4] Bardgett, Gourier, and Leippold (2016) do not account explicitly for a stochastic vol-of-vol, but estimate a model that incorporates a central tendency factor, using VIX and S&P500 option data. Mencia and Sentana (2013) test several models for VIX options, but do not look at the VVIX.

[5] We only know of Lin (2007), who gives an approximation for VIX futures by using the method of Brockhaus and D. (2000) and Bates (2006), which relies on 2^{nd} order Taylor approximations.

Options Exchange (CBOE) computes the VIX index from the entire strike range of out-of-the-money (OTM) S&P500 options via

$$\text{VIX}_t^\tau = 100\sqrt{\frac{2}{\tau}\sum_i \frac{\Delta K_i}{K_i^2}\, e^{r\tau}\, O_t(K_i, t+\tau) - \frac{1}{\tau}\left(\frac{\text{F}_t^{t+\tau}}{K_{ATM}} - 1\right)^2}. \quad (1)$$

O_t are the prices of OTM options with strike prices K_i and $\Delta K_i = \frac{K_{i+1}-K_{i-1}}{2}$ is the interval between strike prices. $\text{F}_t^{t+\tau}$ is the forward price, and K_{ATM} denotes the highest strike price below the forward price of the S&P500. While the last term of Equation (1) is a correction term for the fact that usually no option is directly at the money, the first term under the square root builds upon the seminal work of Demeterfi, Derman, Kamal, and Zou (1999), Britten-Jones and Neuberger (2000), Carr and Madan (1998) and Jiang and Tian (2005). They show that the model-free implied variance (mfVar) equals the price of a portfolio of OTM options with a continuous and infinite strike range, given by

$$\text{mfVar}_t^\tau = \frac{2e^{r\tau}}{\tau}\left[\int_0^{F_t^{t+\tau}} \frac{1}{K^2}\, P_t(K, t+\tau)dK + \int_{F_t^{t+\tau}}^{\infty} \frac{1}{K^2}\, C_t(K, t+\tau)dK\right], \quad (2)$$

where P_t, and C_t are put and call option prices, respectively. Comparing Equation (2) and the first term under the square-root in Equation (1), the CBOE's VIX is clearly subject to approximation errors: The discrete and limited range of option prices leads to the well-known *discretization* and *truncation error*, which we account for explicitly in our empirical analysis.[6,]

Since February 24 2006, European style options are traded on the CBOE VIX index. The availability of various strike prices and the trading volume of VIX options increased steadily after their introduction, illustrated by Figure 1. Especially short-term OTM call options arouse a great deal of interest of market participants. The high availability and liquidity of VIX options allows us to go one step further in terms of studying the implied variance of the VIX itself. Using the CBOE's methodology

[6]For a discussion of approximation errors of the VIX see for example Jiang and Tian (2007).

in Equation (1) for different maturities τ of VIX options gives us the VVIX term structure (VVIX$^\tau$), which serves us as a measure for implied volatility-of-volatility (vol-of-vol) over different time horizons.

Although the VIX and VVIX term structures are available to the public via CBOE's website, we choose to construct the indices ourselves in order to ensure consistency between the empirical analysis and the later model estimation.[7] As such, we use S&P500 options and VIX options in order to build the VIX and VVIX for 30, 60, 90, 120 and 150 days to maturity. Figure 1 shows a limited strike range and low liquidity in the early days of VIX option trading, especially for maturities above 120 days. For this reason we discard the first one and a half years of data and consider the time period from September 1, 2007 to August 29, 2014. This gives us a data set of seven years, including the financial crisis and the peaks of the European sovereign debt crisis. Daily settlement bid-ask prices of S&P500 and VIX options are obtained from Option Metrics. We further use VIX futures quotes from the CBOE. The risk-free rate follows from constant maturity bill yields, which are taken from the Federal Reserve's website.

In line with the methodology of the CBOE for the calculation of the VIX, we filter out all options with zero bids.[8] To reduce the discretization error, we then interpolate the implied volatility surface of VIX options on a finer grid of strike prices via a smoothed cubic spline.[9] Hereby, we force the spline to remain within the bid-ask spread. This procedure is similar to the methodology described e.g. in Carr and Wu (2009) and Jiang and Tian (2005). In contrast to the latter, we do not interpolate only across strikes for the VVIX term structure, but also across

[7] The CBOE publishes the term structure of the VVIX on http://www.cboe.com/publish/vvixtimeseries/vixvixtermstructure.xls.

[8] See CBOE (2009).

[9] We choose $\Delta K = 1$ (in annual volatility points). We find no significant difference in the VVIX term structure for an even finer grid of strike prices. The difference in strike prices is on average roughly 2.5 for all maturities in the data.

maturities. Thereby, we do not straddle the time to maturity of interest in our VVIX construction.[10] We also refrain from extrapolating above the highest available maturity, because it could result in negative implied volatilities. As such, we discard 40 days in our sample period, where no maturity is available for VIX options of at least 150 days. This leaves us with 1721 days of data availability. We then apply Formula (1) to the VIX options, where we neglect the adjustment term, since it becomes negligibly small due to the interpolation in the strike dimension.[11]

The correlation of our $\text{VVIX}^{30\text{D}}$ with the VVIX values reported by the CBOE is 98.7%, implying that our data processing works satisfactorily well.[12] We investigate the empirical descriptives and the predictive power of the VVIX and its term structure in the subsequent chapters. We start by looking at single maturities for VVIX^{τ} first and then summarize the term structure by its principle components.

2.2 VVIX Term Structure Descriptives

The VVIX for 30, 90 and 150 days to maturity is plotted in Figure 2, statistical descriptives are provided in Table 1.[13] While the VIX term structure is upward sloping on most days, the VVIX term structure is downward sloping in nearly all cases. This is expected since the volatility of VIX futures prices (the underlying of the VVIX) is decreasing in their time to maturity.[14] The standard deviation of

[10] This is especially beneficial for our later estimation, since it lowers the computational burden.

[11] We construct the VIX term structure in the same fashion.

[12] The difference between our measure and the CBOE's is not systematic, e.g. not driven by high levels of the VVIX. The quality of the fit to the data is nearly unchanged if we do not interpolate across maturities, but straddle the required maturity. As a robustness check, we also apply the methodology of Bakshi, Kapadia, and Madan (2003) to our data, but find no significant changes in the informational content.

[13] In the plot, we neglect 60 and 120 days of maturity for illustrative purposes.

[14] See for example, Amengual (2008), Luo and Zhu (2010), Luo and Zhang (2012), Huskaj and Nossman (2013) and Ait-Sahalia, Karaman, and Mancini (2015).

$VVIX^{30D}$ is much higher than for longer maturities. Further, we observe an increasing persistence, measured by first order autocorrelations. Also, while the $VVIX^{30D}$ is positively skewed, the distribution of the model-free vol-of-vol for 60 days becomes rather symmetric. For maturities from 90 to 150 days we even observe a slightly left-skewed and platykurtic distribution.

Spikes in the $VVIX^{30D}$ relate to financial and economical meaningful events. For example, the response to the downgrade of the US' credit rating on August 8, 2011 is reflected in a value of the $VVIX^{30D}$ of 143.92. This value is comparable to the spike of 138.49 in the course of the sub-prime crisis on October 27, 2008, when the U.S. Treasury refunded 22 banks with 38 billion dollars in a second round of recapitalization.[15] Furthermore, on May 20 and May 21, 2010, we not only observe a comparable level of the $VVIX^{30D}$, but also the highest levels across all maturities. This reflects the high uncertainty about the proceedings of the crisis of Greece. Noteworthy, the different levels of the VIX suggests that market uncertainty during the turmoils of the European sovereign debt and fiscal cliff crises were not as severe as in the financial crisis of 2008. However, the VVIX shows that uncertainty about volatility was equally high across all three events. This already indicates that both measures carry different information about volatility risks.

In general, for different maturities the VVIX reacts differently to financial and economic conditions. This can be seen from the correlations of log-changes across the term structure and by the correlations between the changes in the term structure and changes of the S&P500 in Table 1. The correlations of changes across the term structure are strictly decreasing for all maturities and can become quite low (0.55), showing that different parts of the term structure carry different pieces of information. As the VIX, the VVIX is negatively correlated to innovations in the S&P500. For 30 to 150 days of maturity the correlation ranges from -0.53 to -0.39. Further,

[15]For a detailed time-line of events in the financial crisis see https://www.stlouisfed.org/financial-crisis/full-timeline.

the table reports that the correlations between innovations in VIX and VVIX are always quite low, ranging from 0.46 to 0.35. All in all, the statistics of the VVIX term structure indicate that different maturities of the model-free implied vol-of-vol carry different economic information, independently of the VIX term structure. Thus, distinct maturities of the VVIX may provide valuable information for researchers and market participants.

Instead of looking at single maturities, we henceforth summarize the VVIX term structure by its principle components. Table 2 shows the resulting PCA components. In line with other studies like Cochrane and Piazzesi (2005), Johnson (2016) and Ait-Sahalia, Karaman, and Mancini (2015), the results in Table 2 allow us to interpret the first (PC1) and second (PC2) principle component as *level* and *slope*, respectively.[16] The level and slope component describe already 98.5% of the variation in the term structure. In comparison to the aforementioned studies, this is slightly less compared to the level and slope component of the term structure for the VIX or for variance swaps.[17] Still, like the other studies on implied return variances, we find that the first two components are the main drivers of the VVIX term structure. While the first two panels of Figure 2 show that the level has a similar trajectory as the $\text{VVIX}^{30\text{D}}$, the bottom panel shows that the slope of the VVIX is distinct. It is quite erratic and peaks at times of market turmoil.

[16]Note that the principle component is normalized to a zero mean. In robustness checks we obtain highly similar results if we use the average of VVIX^{τ} on day t instead of the *level* component and define the *slope* as the difference of the short- and long-end of the term structure divided by the mean of VVIX^{τ}_t.

[17]In Ait-Sahalia, Karaman, and Mancini (2015), PC1 and PC2 explain 99.9% of the variation in the variance swap term structure, Johnson (2016) attributes 99.36% of the variation of the VIX term structure to the level and slope component. For the yield curve Cochrane and Piazzesi (2005) find that the level and slope factor explain 99.94% of its variation.

2.3 Predictive Regressions

Johnson (2016) finds that the slope of the VIX term structure conveys information for future returns, while the level of the VIX does not. As such, he attributes predictive power to the VIX slope for variance investments. Motivated by his findings and the documented differences between the VIX and VVIX term structure, we analyze the informational content of the *level* and *slope* component of the VVIX term structure via predictive regressions. It is well known that delta neutral straddles can be used as efficient hedges against volatility risk, but up to now little is known about the impact of volatility-of-volatility on these products.[18] To study the economic importance of volatility-of-volatility we analyze the predictive power of the level and slope of the VVIX for these straddles. Our goal is to investigate which part of the term structure proxies vol-of-vol risk and in how far it is a risk factor. Therefore, we look at daily excess returns of S&P500 and VIX straddles, because these products are mainly exposed to volatility risks. In particular, S&P500 straddles are subject to volatility and volatility-of-volatility risks, whereas VIX straddles are exposed to volatility-of-volatility risks only.

The daily straddle returns are calculated as the return of a strategy that holds an at-the-money straddle with a maturity τ for exactly one day

$$\mathrm{r}_{t+1}^{\mathrm{Straddle,raw}} \equiv \frac{\frac{T_2-\tau}{T_2-T_1}\mathrm{Straddle}_{t+1}(T_1) + \frac{\tau-T_1}{T_2-T_1}\mathrm{Straddle}_{t+1}(T_2)}{\frac{T_2-\tau}{T_2-T_1}\mathrm{Straddle}_{t}(T_1) + \frac{\tau-T_1}{T_2-T_1}\mathrm{Straddle}_{t}(T_2)} - 1, \tag{3}$$

where $\mathrm{Straddle}_t(T)$ is the price of an at-the-money delta-neutral straddle at time t, which matures at $t+T$. We calculate the returns as explained in Coval and Shumway (2001) using end of day prices at t and $t+1$. We look at S&P500 straddles with maturities of $1, 2, 3, 6, 9$ and 12 months and at VIX straddles with maturities of $1, 2, 3, 4$ and 5 months. We approximate maturity τ by linear interpolation between

[18] See for example Fan, Gupta, and Ritchken (2003), Brenner, Ou, and Zhang (2006), and Ni, Pan, and Poteshman (2008).

the two nearest traded maturities $T_1 \leq \tau \leq T_2$.[19]

In Table 3 we document the median and the first four moments of the daily straddle excess returns $\mathrm{r}_{t+1}^{\text{Straddle}} = \mathrm{r}_{t+1}^{\text{Straddle,raw}} - r_t^f$, where r_t^f is the short rate on day t. In line with Coval and Shumway (2001) the returns for S&P500 straddles are all negative. The mean returns increase from -0.50% for one month to maturity to -0.02% for twelve months to maturity. This implies that market participants are willing to pay an insurance premium, which becomes smaller for longer maturities. Our estimates are highly similar to the findings of Johnson (2016), whose sample already starts in 1996. In comparison, our estimates of the mean and standard deviation are only slightly higher. As expected for hedge products, the skewness of all straddle excess returns is positive and the kurtosis is well above 3. VIX straddle returns are characterized by similar, but higher mean values. Thus, investors pay a lower, but still negative premium for VIX straddles. However, VIX straddles are exposed to a higher standard deviation and kurtosis.

In our main analysis we regress the one-day ahead straddle excess returns $\mathrm{r}_{t+1}^{\text{Straddle}}$ on a vector X_t of predictive variables. We control for possible autocorrelation effects by including the time t straddle excess return $\mathrm{r}_t^{\text{Straddle}}$. As such, the predictive regressions take the form

$$\mathrm{r}_{t+1}^{\text{Straddle}} = \alpha + \beta_1' X_t + \beta_2 \mathrm{r}_t^{\text{Straddle}} + \epsilon_{t+1}, \tag{4}$$

where the predictive variables X_t are normalized by their standard deviation to obtain comparable beta estimates. We concentrate on the one-day horizon to maximize the number of observations in our short sample period and to remain comparable to the results in Johnson (2016). Still, we find that our results hold up to three weeks for S&P500 and one week for VIX straddles as well as for lagged predictors.[20]

[19] Note that we do not use the artificial option data set described in Section 2.1, but real end-of-day option prices to compute the straddle returns.

[20] See Tables O.1 to O.4 in the online appendix.

X_t contains $\text{VVIX}^{30\text{D}}$, $\text{Slope}^{\text{VVIX}}$, which is the second PCA component of the VVIX term structure, $\text{Slope}^{\text{VIX}}$, which is defined as the second PCA component of the VIX term structure, the $\text{VIX}^{30\text{D}}$ and the VRP.[21] Noteworthy, our results are insensitive to whether we choose (V)$\text{VIX}^{30\text{D}}$ or the first principle component as the level component of the term structure. Table 4 reports the descriptives of our predictors. To rule out problems of multicollinearity, it also shows the historical correlations of the predictive variables, which are rather small.

At first, we analyze VIX straddles. Since they are mainly exposed to vol-of-vol risk, VIX straddle returns allow to test if and which part of the VVIX term structure captures vol-of-vol risk. Table 5 shows the results of our regressions for daily VIX straddle returns. We find that excess returns of one-month VIX straddles are hard to predict since none of our variables has predictive power. In contrast, daily straddle returns with maturities between 2 and 5 months can be predicted by $\text{Slope}^{\text{VVIX}}$ with t-statistics well above 3. The sign of $\text{Slope}^{\text{VVIX}}$ is positive. Also the VRP is highly significant for straddles with maturities of more than one month with a negative sign. The level of the VVIX ($\text{VVIX}^{30\text{D}}$) has no predictive power, as well as the level of the VIX ($\text{VIX}^{30\text{D}}$). Likewise, the slope of volatility, $\text{Slope}^{\text{VIX}}$, has no forecasting power. The missing predictive power of the VIX term structure is not surprising since the straddles are (approximately) delta-neutral with respect to the VIX futures price. In sum, we find that $\text{Slope}^{\text{VVIX}}$ and the VRP predict daily returns of VIX straddle for two to five months to maturity with adjusted R^2s ranging

[21] The VRP is calculated as the difference between the risk-neutral and the physical expectation of the variation of the stock index over the next 30 days, $\text{VRP}_t \equiv 12\left(\mathbb{E}_t^{\mathbb{Q}}\int_0^{30\text{D}}(d\ln S_{t+u})^2du - \mathbb{E}_t^{\mathbb{P}}\int_0^{30\text{D}}(d\ln S_{t+u})^2du\right) = \text{VIX}_t^2 - \mathbb{E}_t^{\mathbb{P}}\,\text{RV}_{t+30\text{D}}$. We assume that RV_t is a martingale, i.e. $\mathbb{E}_t^{\mathbb{P}}\,\text{RV}_{t+30\text{D}} = \text{RV}_t = 12\sum_{j=1}^{21}\sum_i(r_{t-j,i})^2$, and $r_{t-j,i}$ are the ith five-minute log-returns at day $t-j$. We obtain the sum of squared realized five-minutes returns from Oxford-Man's database, which can be found under `http://realized.oxford-man.ox.ac.uk`. Our methodology for the VRP estimation is consistent with Bollerslev, Tauchen, and Zhou (2009) and Carr and Wu (2009) among others.

from 1.77% to 4.20%. According to the magnitude of the regressors, $\text{Slope}^{\text{VVIX}}$ is more important for short maturities, while the VRP is more important for straddles with 4 and 5 months to maturity. Overall, the regression of VIX straddle returns shows that the slope and not the level of the term structure captures time-varying vol-of-vol risk.

We now test whether vol-of-vol risk is also priced in S&P500 straddles and thereby has an influence on stock options in general. Table 6 reports the results of predictive regressions for S&P500 straddle returns for all maturities. As for the VIX straddles we find that adjusted R^2s are fairly low with values in the range of 1.35% to 3.94%. Also, neither of both levels, VIX^{30D} and VVIX^{30D}, has any predictive power. In comparison to the VIX straddle returns, we find that the slope of the VIX is now a significant predictor for all maturities at the 5%-significance level. This confirms the results in Johnson (2016), who documents that the VIX term structure is priced in S&P500 straddles. Interestingly, the slope of the VVIX keeps its predictive power also for S&P500 straddles at the 1% level. We even find that it predicts returns at the very short end of maturity. The magnitude of the standardized regressors and t-statistics of $\text{Slope}^{\text{VVIX}}$ are highest amongst all predictors for all maturities. The only exception is the lagged return. The better performance of $\text{Slope}^{\text{VVIX}}$ suggests that vol-of-vol risk is at least as important as volatility risk itself. In all regressions, the coefficient of $\text{Slope}^{\text{VIX}}$ is negative and increases with time to maturity. This means that expected returns of short-term straddles decrease most if the slope of the VIX increases. The coefficient of $\text{Slope}^{\text{VVIX}}$ is positive and decreases in the straddles' time to maturity. Therefore, a steeper $\text{Slope}^{\text{VVIX}}$ predicts higher expected returns for S&P500 straddles.

In order to assess the importance of the different risk factors and to rule out that our results are driven by multicollinearity, we also run restricted regressions. The main results are consistent for all straddles. For the sake of brevity, we therefore

only present the results for daily returns of SPX and VIX straddle returns with a maturity of two months in Table 7.[22] Regressions (1)-(5) are univariate regressions for each of the predictors, including the lagged return to control for autocorrelation. Compared to the full regression in Tables 5 and 6 the sign and significance do not change. Regressing the straddle returns solely on the slope of the VVIX in (2) gives adjusted R^2-values of roughly 1.4% and 0.73% for VIX and SPX straddles, respectively. This is already a big share of the full regression results, where we find 1.8% and 1.4%. Adding the level of the VVIX term structure does not change R^2 values in regressions (6). Similar, the level and slope of the VIX do not add any predictive power for VIX straddles in regression (8). The results are different for S&P500 straddles. There we find that the explanatory power of the VVIX and VIX slope in regression (2) and (3) almost add up to the R^2 of the full model and remain significant in (7), where we include both variables. This stresses that the slopes of the VIX and VVIX term structure proxy distinct risk-factors, whose informational contents are incremental to each other.

All in all, our analysis shows that the slope of the VVIX term structure, not its level, proxies vol-of-vol risk. Our results for VIX straddles indicate that vol-of-vol risk is quite different from volatility risk, since only the slope of the VVIX has predictive power. The results on S&P500 straddles give further evidence for this claim, since both slopes have predictive power on their own and their explanatory powers almost add up in terms of R^2 if both variables are included.

[22] We choose straddles of two months to maturity, because one month VIX straddle returns are hard to predict as outlined above. Restricted regressions for all maturities can be found in the online appendix in Tables O.5 to O.13.

2.4 Trading Signals from the (V)VIX Term Structure

The predictive regressions in the previous section yield highly significant predictors, but rather low R^2 values. For this reason we further study the economic importance of our results. We test a daily long/short S&P500 straddle investment strategy. For each day we calculate $\text{Slope}_t^{\text{VVIX}}$ and $\text{Slope}_t^{\text{VIX}}$ using only information from the beginning of our sample until day t.[23] This means that we calculate the slopes on date t only based on the data sets $\{(\text{V})\text{VIX}_s^\tau\}_{s\leq t}$ up to time t. The analysis thereby does not suffer from a look-ahead bias, but is rather an out-of-sample strategy, which only uses past information. The question is at which times the VIX and VVIX term structure signal a sufficient increase in volatility risk, which leads to a positive straddle premium.

We analyze two strategies which both short the S&P500 straddle as a default action to earn the negative risk premium, documented in Table 3. Motivated by the coefficient's sign in the predictive regressions, the first strategy goes long if $\text{Slope}_t^{\text{VVIX}}$ is above its 75% percentile and the second strategy goes long if $\text{Slope}_t^{\text{VIX}}$ is below its 25% percentile.[24] Figure 3 shows logarithms of the resulting return paths for S&P500 straddles with maturities of one and twelve months versus the short only strategies. Grey areas mark times where the strategies go long in straddles. Using the signal from the VVIX term structure results in significant excess returns for both maturities. Furthermore, the trading signal of the VVIX term structure is evenly spread over time. When the signal from the VIX is used, the long/short strategy performs worse than the short only strategy for one month straddles and outperforms only weakly for longer maturities. Additionally, the times of going long are clustered around the financial crisis and the years after 2012. This shows that the VVIX term

[23] The burn-in phase is one month (September '07).

[24] We tested a similar strategy with the VRP as the trading signal, where we go long if the VRP is below its 25% percentile. Figure O.1 in our online appendix shows that the resulting strategy is comparable to the VIX term structure.

structure is a more suitable and more homogeneous indicator for economic crises than the VIX term structure, since it indicates states of financial distress more reliably.[25] The superiority of the vol-of-vol signal is evident from annualized Sharpe Ratios as well. For straddles of one (twelve) month the short/long strategy based on $\text{Slope}^{\text{VVIX}}$ has an annual Sharpe Ratio of 1.50 (1.09). The short/long strategy based on $\text{Slope}^{\text{VIX}}$ results in much lower ratios of 0.98 (0.51) for the shortest (longest) maturity.[26]

We conduct a similar analysis for two month VIX straddles. The strategy goes long the straddle if $\text{Slope}^{\text{VVIX}}$ (VRP) is in its highest (lowest) quantile and short otherwise. Figure 4 documents the cumulative log-returns of these strategies. Both strategies lead to economic sizable excess returns and annualized Sharpe Ratios of 0.91 (0.78) for the VVIX (VRP) strategy. In comparison, a simple short-only strategy yielded a Sharpe Ratio of 0.61. As the VVIX term structure, the VRP indicates to go long in times of high financial distress, like the financial crisis, European dept crisis and the Fiscal Cliff crisis. However, similar to the trading signals of $\text{Slope}^{\text{VIX}}$ for S&P Straddles, signals from the VRP cluster after 2013. Thus, in contrast to the signals of $\text{Slope}^{\text{VVIX}}$, VRP signals are not evenly spread across time.

In sum, our trading strategies document that the slope of the VVIX term structure not only proxies a significant risk factor in a statistical sense. It shows that vol-of-vol risk is important for stock and volatility options in economic terms, too.

[25] See for example the peaks of the European sovereign debt crisis in 2010 and the American Fiscal Cliff in late 2011.

[26] The short only strategy has Sharpe ratios of 1.26 and 0.26 for maturities of one and twelve months. For comparison, going long the S&P500 would have resulted in a Sharpe Ratio of 0.24. We also conducted the analysis without the longest end of maturity $(\text{V})\text{VIX}^{150\text{D}}$. The occurrence of signals does not change heavily, leading to similar strategy returns. The short-term straddles perform slightly better, the long-term straddles slightly worse.

3 VVIX Decomposition

Our empirical analysis shows that the term structure of volatility-of-volatility matters for future returns on volatility-sensitive assets. The slope of the VVIX is a highly significant predictor for excess returns of S&P500 straddles and VIX straddles. Importantly, it has additional explanatory power compared to other established variance risk measures, especially the slope of the VIX and the VRP. Moreover, the slope of the VVIX seems to be more informative about excess returns than the slope of the VIX. This suggests that options on the stock market index do not only depend on the risk neutral expectation of future changes in the volatility level, but also on its expected variation.

This raises two fundamental questions: First, why does the slope of the VVIX contain valuable information, while the level does not? Second, what does a steeper slope of the VVIX term structure imply economically? To shed some light on the drivers behind the dynamics of the VVIX term structure and its predictive power, we study two possible sources of vol-of-vol risk, continuous volatility-of-volatility and discontinuous variance jumps. Our setting provides an environment to study the VVIX consistent with VIX derivatives.

3.1 Model Setup

In our empirical section we show, consistent with Huang and Shaliastovich (2014), that the dynamics of the $\text{VVIX}^{30\text{D}}$ and the $\text{VIX}^{30\text{D}}$ are almost independent to each other. More importantly, our results show that this feature holds for longer maturities, too. We thus use a model that features explicitly a stochastic vol-of-vol process. Following Duffie, Pan, and Singleton (2000), we focus on an affine model to describe the dynamics of the log stock price s_t, the variance V_t and the volatility-of-volatility

q_t under the risk-neutral measure $\mathbb{Q}$:

$$ds_t = rdt + \sigma_S \sqrt{V_t} dW_t^S \tag{5}$$

$$dV_t = \kappa_V(\bar{V} - V_t)dt + \sigma_V \sqrt{q_t} dW_t^V + Z_V dN_t \tag{6}$$

$$dq_t = \kappa_q(\bar{q} - q_t)dt + \sigma_q \sqrt{q_t} dW_t^q, \tag{7}$$

where κ_V, κ_q, and $\sigma_V, \sigma_q \in \mathbb{R}^+$ are the mean-reversion speeds and the diffusive volatilities, respectively.[27] We fix the mean-reversion levels $\bar{V}$ and $\bar{q}$ at 1. $r \in \mathbb{R}$ is the risk-free rate and W^S, W^V, W^q are Wiener processes with correlation matrix

$$\begin{pmatrix} (dW_t^S)^2 & dW_t^S dW_t^V & dW_t^S dW_t^q \\ dW_t^S dW_t^V & (dW_t^V)^2 & dW_t^V dW_t^q \\ dW_t^S dW_t^q & dW_t^V dW_t^q & (dW_t^q)^2 \end{pmatrix} = \begin{pmatrix} 1 & 0 & 0 \\ 0 & 1 & \rho_{Vq} \\ 0 & \rho_{Vq} & 1 \end{pmatrix} dt. \tag{8}$$

We are primarily interested in analyzing the VVIX and its term structure. We therefore abstract from the leverage effect and from jumps in the stock price, since this would require a joint treatment of variance and equity derivatives, which is not the focus of this paper. We thus restrict ourselves to a stochastic variance V_t of the stock price, which has itself a stochastic volatility q_t. Both V_t and q_t are mean reverting. While q_t is purely diffusive, V_t exhibits jumps with time-varying intensity. N_t is a compound Poisson process with intensity $\lambda_1^V V_t$ for $\lambda_1^V > 0$, and the random jump-size Z_V has an exponential distribution $\text{Exp}(\mu_V)$ with mean jump-size μ_V.[28] We choose a time-varying jump intensity to capture jump clustering in volatilities, which is documented by Eraker, Johannes, and Polson (2003), Daal,

[27] Since we aim to explain the second moment of the VIX distribution, we refrain from other state-variables, as for example a stochastic central tendency either in V or q, which would improve the general fit, but which would also facilitate the estimation a lot. For our purposes, the estimation results show that the model captures the VVIX term structure already quite well.

[28] We choose to couple the jump intensity to the variance level V_t and thus remain in the standard setting of the option pricing literature. Further, we refrain from a constant intensity, because it would lower the volatility of the VIX.

Naka, and Yu (2007) and Zang, Ni, Huang, and Wu (2017). In addition, Branger, Kraftschik, and Völkert (2016) show that a model with stochastic jump intensity fits VIX option prices better than a model with a constant jump intensity, and thus also fits the VVIX better.[29] We summarize the structural model parameters $\kappa_V, \kappa_q, \sigma_V, \sigma_q, \rho_{Vq}, \mu_V$ and λ_1^V in Θ. Further, Y contains the state-variables V and q.

A well-known result for the affine model-class is that the squared $(\text{VIX}_t^\tau)^2$ is an affine function of the state variable V. In our model the VIX_t^τ is thus given by

$$\begin{aligned} \text{VIX}_t^\tau &= \sqrt{A^{\text{VIX}}(\Theta,\tau) + B^{\text{VIX}}(\Theta,\tau)V_t} \quad , \quad \text{with} \qquad (9) \\ A^{\text{VIX}}(\Theta,\tau) &= \frac{\bar{V}\kappa_V}{\kappa_V - \mu_V\lambda_1^V}\left(\sigma_S^2 - B^{\text{VIX}}(\Theta,\tau)\right) \\ B^{\text{VIX}}(\Theta,\tau) &= \frac{1}{\tau}\,\sigma_S^2\,\frac{1-e^{-(\kappa_V-\mu_V\lambda_1^V)\tau}}{\kappa_V-\mu_V\lambda_1^V}. \end{aligned}$$

The underlying of the VVIX is not the VIX, but its log futures price. Thus, the calculation of the VVIX in the model is two-fold troublesome. First, the VIX futures price is the expectation of Equation (9). Second, due to the square root, an exact closed-form affine solution for the VIX futures price, and thus for the VVIX, does not exist. A further obstacle is that the level of the model-implied VIX is clearly independent of the vol-of-vol q.[30] This makes the estimation of the vol-of-vol state-variable much more involved. We address these problems by first calculating the VIX option prices which then give the VVIX term structure. Specifically, we estimate the model in the next section by computing the model's VIX option prices first, and aggregate them to the model-implied VVIX by Equation (1) afterwards. In this way, we can also replicate the truncation and discretization error of the empirical VVIX.

[29] Branger, Kraftschik, and Völkert (2016) further show that exponentially distributed jumps suffice to describe the dynamics of VIX options and that gamma distributed jumps do not enhance the model's performance.

[30] The vol-of-vol matters, however, for the dynamics of the VIX and thus for the pricing of VIX derivatives and the VVIX.

3.2 Model Estimation

To estimate our model, we use weekly data of the VVIX term structure and the underlying VIX option and future prices. In order to minimize the number of holidays in our sample we choose Wednesday data. If, however, no data is available for a specific week, we rely on the next available datapoint.[31] This leaves us with 365 observations for the estimation. Using these datapoints, we estimate the structural model parameters Θ by minimizing the sum of squared errors in the model's term structure of the VVIX $(\mathrm{VVIX}_{t_i}^{\mathrm{M},\tau_j}(\Theta, Y_i))^2$ and in the underlying VIX futures prices $(\mathrm{F}_{t_i}^{\mathrm{M},t_i+\tau_j})$.[32] We look at the relative squared pricing errors in order to give each observation comparable weight in the loss function, which is given by

$$\begin{aligned}\mathrm{relSE} = \min_{\Theta,Y} \frac{1}{2} \sum_{i=1}^{N} \sum_{j=1}^{J=5} &\left[\frac{\left(\mathrm{VVIX}_{t_i}^{M,\tau_j}(\Theta, Y_i)\right)^2 - \left(\mathrm{VVIX}_{t_i}^{\tau_j}\right)^2}{\left(\mathrm{VVIX}_{t_i}^{\tau_j}\right)^2} \times 100 \right]^2 /(5N) \\ &...+ \left[\frac{\mathrm{F}_{t_i}^{\mathrm{M},t_i+\tau_j}(\Theta, Y_i) - \mathrm{F}_{t_i}^{t_i+\tau_j}}{\mathrm{F}_{t_i}^{t_i+\tau_j}} \times 100 \right]^2 /(5N). \end{aligned} \tag{10}$$

The loss function (10) can also be understood as the relative squared error (relSE). A nice feature of this loss function is that the square root of (10), the relative root mean squared error (relRMSE), represents the mean percentage error. As this performance measure is also applicable for the first and second part of (10), as well as for each maturity, it provides an intuitive and consistent evaluation of the model's fit to different maturities. Adding the VIX futures prices to the loss function is of special importance, since the model not only needs to describe the VVIX term structure, but also has to be consistent with the prices of the underlying. The VIX

[31] This can either be due to a holiday or because we discard days which would require to extrapolate above the longest time to maturity. In 18 out of 21 cases, the next available date is a Thursday.

[32] We take the squared VVIX to circumvent problems of imaginary solutions in the optimization.

futures price arises endogenously from the model, which is pivotal for our purposes, since it sets the integration bounds in Equation (2) by defining OTM options.[33]

We estimate the model's parameters and the state variables in a two step procedure, which is similar to the methodology in Bates (2000), Huang and Wu (2004) and Christoffersen, Heston, and Jacobs (2009) among others. In both steps, we use the pricing methodology of Branger, Kraftschik, and Völkert (2016) to obtain the model's VIX futures and option prices underlying the VVIX term structure. Using the VIX option prices we then calculate $\text{VVIX}_{t_i}^{\text{M},\tau_j}$ by Equation (1).[34] Note that we compute the same option prices as those enter the empirical VVIX term structure. We thereby remain consistent with the data, since we deliberately replicate the truncation and discretization error discussed in Section 2.1.

In the first step of our estimation routine, we choose the structural parameters Θ by the differential evolution algorithm of Wang, Zixing, and Zhang (2011), given the state-variables Y. The second step of our optimization routine, the estimation of the state-variables, is much more involved. At each day t_i, we optimize over Y_i with a gradient-based solver, again by minimizing Equation (10), given a parameter set Θ. This optimization problem is, however, possibly ill-posed, meaning that multiple local minima might exist for different combinations of the state variables. This is especially the case if the correlation between q and V becomes very high. To obtain stable and economically sensible results, we proceed as follows. Given the parameter set Θ, we use the empirical level of the $\text{VIX}^{30\text{D}}$ at day t and invert Equation (9) to get an initial value $V_{t,ini}$

$$V_{t,ini} = \frac{\left(\text{VIX}_t^{30\text{D}}\right)^2 - A^{\text{VIX}}(\Theta, 30/365)}{B^{\text{VIX}}(\Theta, 30/365)}. \tag{11}$$

[33] The error of the futures price is further comparable to the penalty term in Andersen, Fusari, and Todorov (2015), which ensures that the estimate of the local variance cannot diverge heavily from economically reasonable values.

[34] As for the empirical VVIX term structure, we neglect the adjustment term, since it becomes negligible due to our fine grid of strike prices.

We then fix $V_{t,ini}$ to get an initial value of $q_{t,ini}$, by optimizing the loss function (10) only with respect to q. Afterwards we jointly estimate V and q, using the previously obtained values as initials to the solver. We iterate the complete estimation routine until no further improvement of the loss function can be achieved. We further apply this optimization procedure multiple times to the data with different starting values for Θ and always obtain identical solutions for the structural parameters and the state vector Y. We thus conclude that our optimization routine works satisfactory well and reliably.

Figure 5 illustrates the quality of the model to describe the data. It shows that the model fits the VVIX term structure and the VIX futures prices quite well. The relative root mean squared errors are reported in Table 8. The relRMSE ranges between 2.63 and 5.16 for the VVIX term structure and between 2.01 and 6.54 for the VIX futures. Interpreted as mean percentage errors, these values are fairly low.

The upper panel of Table 8 reports parameter estimates Θ and their standard errors. The latter are very narrow, showing that our estimates are very precise, due to the broad cross-section of derivative prices we use in the estimation routine.

3.3 VVIX Approximation

To analyze the VVIX by decomposing it into different risk factors, a proper closed-form representation is needed. In the stochastic volatility-of-volatility market model, which we introduced in Section 3.1, such a closed form representation does not exist. In this chapter we will first explain the basics of a methodology to come up with an affine approximation for the VVIX for different times to maturity. Afterwards we employ the described method to our model setting and validate its accuracy via a simulation exercise.

3.3.1 The Approximation – A Brief Introduction

In this section, we explain the steps which are necessary to approximate the VVIX term structure in closed form only briefly. Details are provided in Appendix A. The VVIX_t^τ at time t for some maturity τ is the square root of the annualized estimated log variation of the VIX futures price with maturity in $t+\tau$ over the horizon t to $t+\tau$. Therefore,

$$(\text{VVIX}_t^\tau)^2 = 100^2 \frac{1}{\tau} \mathbb{E}_t^{\mathbb{Q}} \left[\int_t^{t+\tau} (d \ln \text{F}_s^{t+\tau})^2 \right], \tag{12}$$

where $\mathbb{Q}$ is the risk-neutral measure and $\text{F}_s^{t+\tau}$ is the VIX futures price at time s with maturity at time $t+\tau$ defined as

$$\text{F}_s^{t+\tau} = \mathbb{E}_s^{\mathbb{Q}} \left[\text{VIX}_{t+\tau}^{30\text{D}} \right]. \tag{13}$$

In general affine asset pricing models it holds that

$$\text{VIX}_t^\tau = \sqrt{A^{\text{VIX}}(\Theta, \tau) + B^{\text{VIX}}(\Theta, \tau)' Y_t}, \tag{14}$$

for $A^{\text{VIX}}(\Theta, \tau) \in \mathbb{R}$, $B^{\text{VIX}}(\Theta, \tau) \in \mathbb{R}^n$ and some vector of state variables $Y_t \in \mathbb{R}^n$. The square root, together with its expectation in (13) and the logarithm in (12), causes serious problems when it comes to calculating VVIX_t^τ and its dynamics. We employ a two step approximation method to overcome these problems. First, we approximate the square root (14) using a second order Taylor approximation which enables us to calculate the futures price (13) in closed form. In the second step, we approximate the log-dynamics (12) using Itô's lemma. Our overall approximation then gives us

$$(\text{VVIX}_t^\tau)^2 \approx A^{\text{VVIX}}(\Theta, \tau, y_t) + B^{\text{VVIX}}(\Theta, \tau, y_t)' \widetilde{Y}_t, \tag{15}$$

where $\widetilde{Y} = [V^3, V^2 q, V^2, q^2, V q, V, q]'$. The expression for the VVIX^2 has a similar structure as for the VIX^2 in Equation (14). However, there are two important differences. First, (15) is an affine function of some (new) state variables $\widetilde{Y}_t$, i.e. the

(old) state variables q, V, their product and some higher cross-moments. Second, it also depends on a set of parameters $y_t \in \mathbb{R}^3$, which arise from the Taylor approximation of the square-root in Equation (14). Since we aim at a high accuracy, we recalibrate y at each day t. So in contrast to A^{VIX} in Equation (9), $A^{\text{VVIX}}(\Theta, \tau, y_t)$ is time-varying. As we show in Appendix A.7, it can be understood as a constant plus a residual component that arises due to non-linear terms of V_t^{-1} and q_t. The latter are not captured explicitly by our approximation method and cannot be incorporated in a way that allows for a closed-form solution. So we do not decompose $A^{\text{VVIX}}(\Theta, \tau, y_t)$ any further. Appendix A.7 also demonstrates that $A^{\text{VVIX}}(\Theta, \tau, y_t)$ can alternatively be interpreted as a different approximation for the VVIX, which ignores higher dimensions of the state variables and is thus less accurate than our approach. In this sense, $A^{\text{VVIX}}(\Theta, \tau, y_t)$ allows us to evaluate the need to account for higher moments. For reasons of readability, we henceforth abbreviate $A^{\text{VVIX}}(\Theta, \tau, y_t)$ and $B^{\text{VVIX}}(\Theta, \tau, y_t)$ with A^{VVIX} and B^{VVIX}, respectively.

Our representation enables us to decompose the VVIX term structure into the contributions of state variables $\widetilde{Y}$. After further sorting for different parameters, we can then differentiate between the loadings on jump risk and diffusive risk.

3.3.2 Accuracy of the VVIX Approximation

To test whether the resulting approximation for the VVIX and its term structure works with desired accuracy, we assess its performance for each Wednesday from 09/01/2007 to 08/31/2014. Doing so, it is important to consider again the truncation and discretization error of the empirical VVIX term structure. In the model estimation, we account for these errors explicitly by relying on the VIX options the VVIX computation is based on. In contrast, the approximation is based on a continuous and unlimited strike range. Thus, when plugging our parameter estimates into the approximation, the resulting VVIX will differ from its empirical counterpart.

We thus compare the approximation with a simulated VVIX ($\text{VVIX}^{\tau,\text{sim}}$), which does not rely on the VIX option prices, but is obtained via Monte Carlo simulation. Specifically, we simulate the futures' price paths at each day t and compute its expected variation. We provide details in Appendix A.6.

The resulting relative errors of the approximation for the VVIX term structure are defined as

$$\epsilon^{\tau}_{\text{VVIX}} \equiv \frac{\sqrt{A^{\text{VVIX}} + B^{\text{VVIX}\prime}\widetilde{Y}_t}}{\text{VVIX}^{\tau,\text{sim}}_t} - 1.$$

Table 9 gives the mean relative errors and standard deviations for maturities ranging from one month to five months. The simulation exercise shows that the approximation is quite accurate since the mean pricing error never exceeds 2.12% in absolute terms. We find a mean error of 0.77% for the shortest maturity of one month. For longer maturities the error increases only slightly and reaches 2.12% for five months. The standard deviations are slightly increasing from 1.23% for one month to maturity to 2.29% for five months. Overall, we conclude that the approximation is rather stable for different maturities and works especially in crisis periods.[35]

3.4 Average Loadings of the VVIX Term Structure

The approximation we propose in Equation (15) enables us to gain further insights about the drivers of the VVIX and its term structure. This can simply be done by decomposing B^{VVIX} into its diffusive and jump parts, which we mark by the superscripts c and j, respectively

$$B^{\text{VVIX}} = B^{\text{VVIX},c} + B^{\text{VVIX},j}. \tag{16}$$

We do the sorting by distinguishing between terms which depend on the model's jump parameters μ_V and λ_1^V ($B_t^{\text{VVIX},j}$) and those which do not ($B_t^{\text{VVIX},c}$). This leads

[35]The relative error over time is plotted in the online appendix, Figure O.2.

to the following decomposition of the VVIX^2

$$(\text{VVIX}_t^\tau)^2 = A^{\text{VVIX}} + B^{\text{VVIX},c'}\widetilde{Y}_t + \underbrace{B^{\text{VVIX},j'}\widetilde{Y}_t}_{\text{JumpRisk}_t^\tau}. \tag{17}$$

Expectations of purely diffusive risks are captured by the vector $B^{\text{VVIX},c}$ multiplied by the vector of state variables $\widetilde{Y}_t$. The average variance jump expectation over period t to $t+\tau$ is captured in JumpRisk_t^τ and is calculated as $B^{\text{VVIX},j'}\widetilde{Y}_t$.[36]

In the following, we look at the composition of the VVIX term structure more closely. We define the contribution of a factor X at time t as

$$W_t^\tau(X) \equiv B_X^{\text{VVIX},c} X_t \tag{18}$$

and the contribution of the jump factor and of the lower bound at time t as

$$W_t^\tau(\text{Jump}) \equiv \text{JumpRisk}_t^\tau \text{ and } W_t^\tau(A^{\text{VVIX}}) \equiv A^{\text{VVIX}}. \tag{19}$$

Further, we define the relative weight of a risk factor as

$$\omega_t^\tau(\bullet) \equiv \frac{W_t^\tau(\bullet)}{(\text{VVIX}_t^\tau)^2}. \tag{20}$$

Over the time-span from 09/2007 to 08/2014 we find that the main drivers are the diffusive volatility-of-volatility component q_t, jump risk and A^{VVIX}. These factors together explain on average over 95% of the VVIX^τ for each maturity τ. In the following, we will therefore only concentrate on the three aforementioned factors.

The average relative weights of the VVIX^τs' most important risk factors are displayed in Figure 6. It reveals an almost linear relationship between the relative

[36] One could (falsely) suspect that the JumpRisk_t^τ stems only from $B^{\text{VVIX},j'}V_t$, since the intensity of the jump process N_t is given by $\lambda_1^V V_t$. Importantly, this is only the local jump intensity of V_t. For the computation of the VIX futures price, and thus for the VVIX, the dynamics of the jump intensity matter. As a result, JumpRisk_t^τ does not only depend on V_t. Details are given in Appendix A.1.

weight of the factors and maturity τ. The impact of continuous vol-of-vol q_t decreases in τ from roughly 55% to 40%. As a result $\text{VVIX}^{30\text{D}}$ depends mainly on continuous volatility-of-volatility risk. Volatility jump risk is the second most important factor, which, on average, decreases only slightly in τ and accounts for around 26%-29% across all maturities. Finally, A^{VVIX} gains importance in maturity since its relative contribution rises from less than 10% to over 29%. These low values show that it is important to account for higher dimensions in the approximation for all maturities.

3.5 The Variance-of-Variance to Variance Ratio

The contribution of continuous vol-of-vol, jump risk and A^{VVIX} depends on the economic condition and thus varies over time. In our model we capture variance risk by the variance-of-variance (q) and variance (V). The top panel of Figure 7 shows the model-implied $\text{VVIX}^{30\text{D}}$ for different pairs of our state variables. The impact of q clearly depends on the level of V. For low values of V the VVIX increases in q, whereas for high values of V vol-of-vol has almost no impact.[37] As we will show, the term structure can be well described by the ratio of our state variables, namely the q/V-ratio. To look at the ratio is rather natural from another point of view as well. A given variance (q) can only be interpreted correctly if it is put in relation to the current level (V).

In the middle panel of Figure 7 we confirm the strong link between our model implied q/V-ratio and the empirical VVIX^{τ}s. The plot scatters the VVIX for the longest and shortest maturity on the ratio. In general we find an almost linear

[37] To get an intuition for the dependence of the VVIX on V and q, remember that by Ito's Lemma

$$(\text{VVIX}_t^{\tau})^2 = \frac{1}{\tau}\mathbb{E}_t^{\mathbb{Q}}\left[\int_t^{t+\tau}(d\ln \text{F}_s^{t+\tau})^2\right] \approx \frac{1}{\tau}\frac{\mathbb{E}_t^{\mathbb{Q}}\left[\int_t^{t+\tau}(d\text{F}_s^{t+\tau})^2\right]}{\left(\text{F}_t^{t+\tau}\right)^2}.$$

Note that $\text{F}_t^{t+\tau}$ is highly dependent on V_t, whereas its expected variation in the nominator is mainly driven by q. See Appendix A.1.

relationship between q/V and the VVIX across all maturities. The effect of the ratio is by a factor of more than two stronger for the short end, compared to the long end of the term structure. This systematic impact of the q/V-ratio on different maturities of the VVIX provides a convenient way to describe the term structure.

The bottom panel of Figure 7 shows the q/V-ratio over time.[38] The ratio behaves countercyclically. Prior to periods of distress, the ratio was below its mean and spiked up to 80% if a crisis hit. In calm times, the variance-of-variance was less than 40% of the variance level and even dropped below 20% in 2014.

4 Dynamics of the VVIX Term Structure

4.1 Drivers of the Term Structure: Why looking at the Slope?

In the previous chapter we have shown that the q/V-ratio is an adequate measure to study the VVIX term structure systematically. Figure 8 displays three different quantities for continuous vol-of-vol, variance jumps and A^{VVIX}, as a function of the q/V-ratio: The left and middle column give the absolute and relative contributions for the shortest and longest maturity. The right column gives each component's contribution to the slope of the term structure, normalized by the local level of the term structure.[39]

For very low realizations of the q/V-ratio, continuous vol-of-vol risk is rather low in relative and absolute terms. In these states of the economy, the jump factor and A^{VVIX} basically determine VVIX^τ. The relative and absolute weights of jumps decrease in maturity, whereas the impact of A^{VVIX} increases. For the slope contri-

[38] In the plot we scale the q/V-ratio by $\sigma_S^2\sigma_V^2$, which is necessary to obtain empirically plausible values, since we fix the mean-reversion levels $\bar{V}$ and $\bar{q}$ in the model estimation.

[39] We compute the slope contribution by $\left(W_t^{30\text{D}}(X) - W_t^{150\text{D}}(X)\right)/\overline{\text{VVIX}_t^M}$. The definition is motivated from the approximation for the second principle component in Section 2.2.

butions shown in the right panels, the positive effect of jumps and negative effects of A^{VVIX} offset each other, which gives a flat slope if q/V is low.

If q/V increases, the relative contribution of A^{VVIX} deteriorates quickly from 50% (70%) at the short- (long) end of maturity to 10% (20%). The negative contribution to the slope goes to zero and vanishes for large values of q/V. We observe a similar pattern for the jump contributions: The relative weights decrease from 45% (30%) at the short- (long) end of maturity to 15% (10%). The absolute jump contribution to the long- and short-end of the term structure is at first roughly stable. For very high q/V-ratios, however, the absolute jump contributions converge. As such, variance jump expectations contribute to the slope if q/V is low. In contrast, if q/V is high, jumps contribute to the level. This is also reflected in the slope contributions of jumps in the right panel. In comparison to the slope contribution of A^{VVIX}, the convergence to almost zero is slower.

The plot for the relative weights of q shows that as soon as q/V increases, the relative importance of continuous vol-of-vol risk rises rapidly from nearly 0% to more than 60% at the short- and long end of maturity. Starting from zero, the absolute contributions grow rapidly as well. This increase is stronger for the short end than for the long-end. The widening spread of short- and long-term contributions transfers into an increase of q's contribution to the slope. Consequently, q does not contribute to the slope at very calm states of the market, but gains importance quickly for medium and large of q/V. At and above the average value of the q/V-ratio, it is the main driver of the slope.

Altogether, our analysis shows that the slope of the VVIX is strongly connected to the state of the economy, measured by the q/V-ratio. In calm times (low q/V) jump expectations drive the slope whereas in times of distress (high q/V) the slope is driven by innovations in q.

4.2 Why not looking at the Level?

The preceding section shows that a steeper (i.e. more negative) slope coincides with larger diffusive vol-of-vol risk. In addition, our predictive regression analysis shows that $\text{Slope}^{\text{VVIX}}$ conveys forward looking information. To give an economic intuition for the predictive power of the slope of the VVIX term structure, we now look at the time-periods around the three biggest crises in our data sample.[40] This is when $\text{Slope}^{\text{VVIX}}$ was highly informative to investors, since it predicted an increase in volatility-of-volatility as shown by the demonstrated returns of our out-of-sample investment strategy in Section 2.4.

Figure 9 refers to the times around the financial crisis of 2008 (left panels), the European Sovereign Debt Crisis (middle panels) and the Fiscal Cliff Crisis (right panels). In each plot the time span starts one month in advance of the first trading signal from $\text{Slope}^{\text{VVIX}}$ that preceded each crisis. This point in time is marked by the first vertical line. The second vertical solid line marks the day when the $\text{VVIX}^{30\text{D}}$ peaked, and we consider the subsequent trading month. The first three panels show the short- and long-end of VVIX^{τ} as well as its level and slope. Importantly, the dashed horizontal line in the level and slope plots are the time-dependent 75% percentile. For the slope panels this line refers to our trading signal in Section 2.4.[41] The lower three panels contain the relative contributions of vol-of-vol risk, jump risk and A_t^{VVIX} to the short- and long-end to the term structure.

The panels for each of the three periods of market stress show basically the same patterns. With the beginning of market turmoil, the level and slope of the VVIX term structure both increase over their 75% percentile. For the financial crisis of 2008, the slope hits its critical value a little earlier than the level, but basically the

[40] To infer the state-variables at these times, we apply our weekly estimates to daily data.

[41] Note that we calculate the level and slope by a rolling-window approach as for our trading strategy in Section 2.4 to preserve the out-of-sample character of the analysis.

level and slope of the VVIX term structure co-move at the crises' beginning. Thus, the level of the term structure also provides valuable information to investors, but *only in advance* of the crisis. The difference between the level and slope shows at and after the peak of market turmoil, marked by the second solid line. While the slope decreases quickly afterwards and falls below its 75% percentile, the level of the VVIX remains at high levels and does not fall below its critical threshold. For a long-short strategy, this tells investors to keep a long position in volatility. But after the peak, vol-of-vol declines, which implies negative daily straddle returns. This drives the wedge between the informational power of level and slope. The preceding gains from trading volatility due to the level signal are annihilated by staying long too long. Stated differently, the level of the term structure is too sticky after market turmoil.[42] In contrast, the slope reaches its highest values before the $\text{VVIX}^{30\text{D}}$ peaks. Its quick decline under its critical quantile prevents that recent trading gains evaporate in the aftermath of the crises' high.

Finally, the risk-(de)composition plots in the lower three rows of Figure 9 give an economic intuition for the information conveyed by the behavior of $\text{Slope}^{\text{VVIX}}$. For all weights, the panels show a transition phase in the risk composition of the term structure from jump risk to continuous vol-of-vol risk. The shifts start roughly at the first trading signal (left vertical line), and finalize when slope leaves its highest quintile (right vertical line).[43] Afterwards, weights are rather persistent and only start very slowly to revert back to former levels. This coincides with the stickiness of the term structure's level.

Figure 9 shows further that during the shift, the relative jump weights are

[42] As a robustness test, we also tried other quantiles for the signal, which softens the stickiness. Then positive returns at the beginning of the crisis are not realized, similar to the short-only strategy. This would leave the level of the term structure as a non-informative signal for investors.

[43] A slight exception is the financial crisis in 2008, but this crisis is not as well matched by our model as the other two.

almost indistinguishable for all VVIX^τ. In 2008 (2010 and 2011), the relative jump contribution drops from 40% (30%) to approximately 20%. In contrast, the diffusive vol-of-vol risk is highly distinct at the long- and short-end of the term structure before the crises. In the progression of the shift, the relative short- and long-term weights of q converge and the diffusive part of vol-of-vol risk rises to more than 60% across the whole term structure. Taking both risk components together, this means that the crises were expected (or at least priced) by market participants: When jump expectations indeed realized, diffusive vol-of-vol risk took over, meaning that volatility became highly uncertain. The similar composition of the short- and long-end of the term structure implies that investors expected this not to change soon.

5 Conclusion

This paper provides a thorough analysis of the term structure of the model-free implied volatility-of-volatility (VVIX^τ). First, we document that the slope of VVIX^τ, not its level, is a significant proxy for vol-of-vol risk. Regressions show that a steepening slope of the VVIX predicts daily straddle returns on the S&P500 and VIX with a positive sign. Most importantly, the informational content of VVIX's slope is distinct and incremental to the VRP as well as to the slope of the VIX. This shows that vol-of-vol risk is an important risk factor not only for VIX options, but for stock index options as well. We demonstrate that a simple out-of-sample trading strategy, which is based on VVIX^τ performs much better than a trading strategy that relies on the VIX term structure or the VRP.

To answer the question which part of vol-of-vol risk is captured by the slope of the VVIX, continuous vol-of-vol risk or jump risk, we set up a full market model which features both types of risk. We then develop a new, higher order approximation method to express the model-implied VVIX as an affine function of the state

variables. This helps us to decompose the VVIX term structure in an intuitive way. We find that the contributions of continuous vol-of-vol and jump risk to the slope vary systematically with the state of the economy, which we capture by the variance-of-variance to variance ratio (q/V). The q/V-ratio is countercyclical. If its value is low, i.e. in calm market states, mainly jump expectations and a constant (plus a residual term) determine the VVIX across all maturities. As their contributions to the slope offset each other, the resulting VVIX term structure is flat. In times of market turmoil (high q/V-ratio), the slope of the term structure is steep and mainly driven by continuous vol-of-vol risk.

Finally, we study the three biggest market downturns of the last decade. Our results show that the slope of the VVIX captures a transition phase for the composition of aggregate vol-of-vol risk. Preceding the crises, jump risk was highly important. When the crises surged, jump expectations played a lesser role in a relative sense and volatility uncertainty took over as the main driver of the VVIX. For the three crises, our findings suggest that market participants expected volatility to remain highly uncertain for a long time.

A Mathematical Appendix

A.1 The VVIX Approximation in more Detail

To approximate the square root in Equation (14), we approximate the VIX dynamics by employing the Babylon method of second order.[44] The approximation gives for some $a > 0$

$$\sqrt{a} \approx \frac{1}{4} y_0 + \frac{1}{4y_0} a + \frac{y_0 a}{y_0^2 + a}, \tag{A.1}$$

where y_0 is an initial guess for the square root of a. We simplify $\frac{y_0 a}{y_0^2+a}$, using a Taylor-approximation around a_0 of second order to obtain a more affine structure, which is given by

$$\begin{aligned}\sqrt{a} \approx f_{a_0,y}(a) \equiv & \frac{1}{4} y_0 + \frac{1}{4y_1} a + \frac{a_0 y_0}{y_0^2 + a_0} \\ & + \frac{y_1^3}{(y_1^2 + a_0)^2}(a - a_0) - \frac{y_2^3}{(y_2^2 + a_0)^3}(a - a_0)^2,\end{aligned} \tag{A.2}$$

where the y_1 and y^2 may be different from y_0. Since all variables are estimated later on, the variability in the y_i is introduced for a higher degree of flexibility in the later calibration procedure. In Appendix A.2 we then show that the approximated futures price $\mathrm{F}_s^{t+\tau}$ is given in affine form by

$$\mathrm{F}_s^{t+\tau} = \mathbb{E}_s^{\mathbb{Q}} \mathrm{VIX}_{t+\tau} \approx \beta_{VV}^{\text{fut}}(\tau(s)) V_s^2 + \beta_V^{\text{fut}}(\tau(s)) V_s + \beta_q^{\text{fut}}(\tau(s)) q_s + \alpha^{\text{fut}}(\tau(s)) \tag{A.3}$$

and that its quadratic variation has the form

$$\mathbb{E}_t \int_t^{t+\tau} \left(d\mathrm{F}_s^{t+\tau}\right)^2 = A^{\langle \text{fut} \rangle}(\Theta, \tau, y, a_0) + B^{\langle \text{fut} \rangle}(\Theta, \tau, y, a_0)' \widetilde{Y}_t, \tag{A.4}$$

where $A^{\langle \text{fut} \rangle}(\Theta, \tau, y, a_0) \in \mathbb{R}$ and $B^{\langle \text{fut} \rangle}(\Theta, \tau, y, a_0) \in \mathbb{R}^m$ are depending on $a_0 \in \mathbb{R}$ and $y \equiv (y_0, y_1, y_2) \in \mathbb{R}^3$. If we use the above approximation together with[45]

$$\int_0^t (d \ln X_s)^2 \approx \widehat{\frac{1}{X_t^2}} \int_0^t (dX_s)^2, \tag{A.5}$$

[44] For historical background and derivation see for example Fowler and Robson (1998).

[45] The approximation can be directly deduced using Itô's lemma

$$d \ln X_t = \frac{1}{X_t} dX_t - \frac{1}{2} \frac{1}{X_t^2} (dX_t)^2,$$

which leads to $(d \ln X_t)^2 = \frac{1}{X_t^2} (dX_t)^2$.

we can calculate the square of VVIX_t^τ in closed-form and obtain

$$\begin{aligned}(\mathrm{VVIX}_t^\tau)^2 &\approx A^{\mathrm{VVIX}}(\Theta,\tau,y,a_0) + B^{\mathrm{VVIX}}(\Theta,\tau,y,a_0)'\widetilde{Y}_t, \\ &\equiv \widehat{\frac{1}{(\mathrm{F}_t^{t+\tau})^2}} A^{\langle\mathrm{fut}\rangle}(\Theta,\tau,y,a_0) + \widehat{\frac{1}{(\mathrm{F}_t^{t+\tau})^2}} B^{\langle\mathrm{fut}\rangle}(\Theta,\tau,y,a_0)'\widetilde{Y}_t.\end{aligned} \tag{A.6}$$

where $A^{\mathrm{VVIX}}(\Theta,\tau,y,a_0) \in \mathbb{R}$ and $B^{\mathrm{VVIX}}(\Theta,\tau,y,a_0) \in \mathbb{R}^m$ are depending on $a_0 \in \mathbb{R}$ and $y \equiv (y_0,y_1,y_2) \in \mathbb{R}^3$. Since we fix a_0 at 1 in the calibration in Appendix A.3, we drop a_0 in the main text.

A.2 Calculation of the Expected Quadratic Variation of the Approximated VIX Futures Price

First, we show that the approximated VIX futures price is given by

$$\mathrm{F}_s^{t+\tau} = \mathbb{E}_s^{\mathbb{Q}}\mathrm{VIX}_{t+\tau}^{30\mathrm{D}} \approx \beta_{VV}^{\mathrm{fut}}(\tau(s))V_s^2 + \beta_V^{\mathrm{fut}}(\tau(s))V_s + \beta_q^{\mathrm{fut}}(\tau(s))q_s + \alpha^{\mathrm{fut}}(\tau(s)). \tag{A.7}$$

We calculate the coefficients using (A.2) and $\left(\mathrm{VIX}_t^{30\mathrm{D}}\right)^2 = A^{\mathrm{VIX}} + B^{\mathrm{VIX}}V_t$

$$\begin{aligned}\mathrm{VIX}_t^{30\mathrm{D}} = \sqrt{\left(\mathrm{VIX}_t^{30\mathrm{D}}\right)^2} \approx f_{a_0,y}\left(\left(\mathrm{VIX}_t^{30\mathrm{D}}\right)^2\right) &= \frac{1}{4y_0} + \frac{a_0y_0}{y_0^2+a_0} + \frac{y_1^3}{y_1^2+a_0}(A^{\mathrm{VIX}}-a_0) \\ &- \frac{y_2^3}{(y_2^3+a_0)^3}(A^{\mathrm{VIX}}-a_0)^2 + \frac{1}{4y_1}A^{\mathrm{VIX}} \\ &+ \left(\frac{y_1^3}{(y_1^2+a_0)^2} + \frac{1}{4y_1} - \frac{y_2^3}{(y_2^3+a_0)^3}2(A^{\mathrm{VIX}}-a_0)\right)B^{VIX}V_t \\ &- \frac{y_2^3}{(y_2^3+a_0)^3}(B^{\mathrm{VIX}})^2V_t^2,\end{aligned}$$

where we write $A^{\mathrm{VIX}} = A^{\mathrm{VIX}}(\Theta,30\mathrm{D})$ and $B^{\mathrm{VIX}} = B^{\mathrm{VIX}}(\Theta,30\mathrm{D})$ for brevity. Hence

$$\mathrm{VIX}_t^{30\mathrm{D}} \approx \beta_{VV}^{\mathrm{VIX}}V_t^2 + \beta_V^{\mathrm{VIX}}V_t + \alpha^{\mathrm{VIX}}.$$

Below we show that one can write

$$\begin{aligned}\mathbb{E}_0^{\mathbb{Q}}V_t^2 &= \beta_{VV}^{VV}(t)V_0^2 + \beta_V^{VV}(t)V_0 + \beta_q^{VV}(t)q_0 + \alpha^{VV}(t), \\ \mathbb{E}_0^{\mathbb{Q}}V_t &= \beta_V^{V}(t)V_0 + \alpha^{V}(t), \\ \mathbb{E}_0^{\mathbb{Q}}q_t &= \beta_q^{q}(t)q_0 + \alpha^{q}(t),\end{aligned}$$

for appropriate $\beta_{VV}^{VV}(t), \beta_{V}^{VV}(t), \beta_{V}^{V}(t), \beta_{q}^{q}(t), \alpha^{VV}(t), \alpha^{V}(t), \alpha^{q}(t) \in \mathbb{R}$. Therefore we define

$$\begin{aligned}
\beta_{VV}^{\text{fut}}(\tau(s)) &\equiv \beta_{VV}^{\text{VIX}}\beta_{VV}^{VV}(\tau(s)),\\
\beta_{V}^{\text{fut}}(\tau(s)) &\equiv \beta_{VV}^{\text{VIX}}\beta_{V}^{VV}(\tau(s)) + \beta_{V}^{\text{VIX}}\beta_{V}^{V}(\tau(s)),\\
\beta_{q}^{\text{fut}}(\tau(s)) &\equiv \beta_{VV}^{\text{VIX}}\beta_{q}^{VV}(\tau(s))),\\
\alpha^{\text{fut}}(\tau(s)) &\equiv \beta_{VV}^{\text{VIX}}(\alpha^{VV}(\tau(s)) + \alpha^{q}(\tau(s))) + \beta_{V}^{\text{VIX}}\alpha^{V}(\tau(s)) + \alpha^{\text{VIX}},
\end{aligned}$$

where $\tau(s) \equiv t + \tau - s$ is the time to maturity of the future $\mathrm{F}_s^{t+\tau}$. From Equation (A.7) follows for the quadratic variation of the approximated futures price

$$\begin{aligned}
\mathbb{E}_t^{\mathbb{Q}} \int_t^{t+\tau} (d\mathrm{F}_s^{t+\tau})^2 = &\int_t^{t+\tau} \mathbb{E}_t^{\mathbb{Q}}(d\beta_{VV}^{\text{fut}}(\tau(s))V_s^2)^2 + \int_t^{t+\tau} \mathbb{E}_t^{\mathbb{Q}}(d\beta_{V}^{\text{fut}}(\tau(s))V_s)^2\\
&+ \int_t^{t+\tau} \mathbb{E}_t^{\mathbb{Q}}(d\beta_{q}^{\text{fut}}(\tau(s))q_s)^2\\
&+ 2\int_t^{t+\tau} \mathbb{E}_t^{\mathbb{Q}}(d\beta_{V}^{\text{fut}}(\tau(s))V_s)(d\beta_{VV}^{\text{fut}}(\tau(s))V_s^2)\\
&+ 2\int_t^{t+\tau} \mathbb{E}_t^{\mathbb{Q}}(d\beta_{q}^{\text{fut}}(\tau(s))q_s)(d\beta_{V}^{\text{fut}}(\tau(s))V_s)\\
&+ 2\int_t^{t+\tau} \mathbb{E}_t^{\mathbb{Q}}(d\beta_{q}^{\text{fut}}(\tau(s))q_s)(d\beta_{VV}^{\text{fut}}(\tau(s))V_s^2).
\end{aligned}$$

Here we can swap the expectations with the integrals since $(d\mathrm{F}_s^{t+\tau})^2 > 0$. Further, Itô gives

$$\begin{aligned}
d\beta_{VV}^{\text{fut}}(\tau(s))V_s^2 &= \frac{d}{dt}\beta_{VV}^{\text{fut}}(\tau(s))V_s^2 dt + \beta_{VV}^{\text{fut}}(\tau(s))dV_s^2 + \ldots dt\\
d\beta_{V}^{\text{fut}}(\tau(s))V_s &= \frac{d}{dt}\beta_{V}^{\text{fut}}(\tau(s))V_s dt + \beta_{V}^{\text{fut}}(\tau(s))dV_s + \ldots dt\\
d\beta_{q}^{\text{fut}}(\tau(s))q_s &= \frac{d}{dt}\beta_{q}^{\text{fut}}(\tau(s))q_s dt + \beta_{q}^{\text{fut}}(\tau(s))dq_s + \ldots dt.
\end{aligned}$$

Hence, since the $\ldots dt$ terms are of finite variation we get

$$\begin{aligned}\mathbb{E}_t^{\mathbb{Q}} \int_t^{t+\tau} (d\mathrm{F}_s^{t+\tau})^2 = &\int_t^{t+\tau} (\beta_{VV}^{\mathrm{fut}}(\tau(s)))^2 \mathbb{E}_t^{\mathbb{Q}}(dV_s^2)^2 \\ &+ \int_t^{t+\tau} (\beta_{V}^{\mathrm{fut}}(\tau(s)))^2 \mathbb{E}_t^{\mathbb{Q}}(dV_s)^2 \\ &+ \int_t^{t+\tau} (\beta_{q}^{\mathrm{fut}}(\tau(s)))^2 \mathbb{E}_t^{\mathbb{Q}}(dq_s)^2 \\ &+ 2\int_t^{t+\tau} \beta_{V}^{\mathrm{fut}}(\tau(s))\beta_{VV}^{\mathrm{fut}}(\tau(s)) \mathbb{E}_t^{\mathbb{Q}}(dV_s dV_s^2) \\ &+ 2\int_t^{t+\tau} \beta_{q}^{\mathrm{fut}}(\tau(s))\beta_{V}^{\mathrm{fut}}(\tau(s)) \mathbb{E}_t^{\mathbb{Q}}(dq_s dV_s) \\ &+ 2\int_t^{t+\tau} \beta_{q}^{\mathrm{fut}}(\tau(s))\beta_{VV}^{\mathrm{fut}}(\tau(s)) \mathbb{E}_t^{\mathbb{Q}}(dq_s dV_s^2).\end{aligned} \tag{A.8}$$

In the following ODEs we calculate the expected values $\mathbb{E}_0 X_t$ relative to the starting time $t_0 = 0$ to ease up notations. However, they can be canonically translated to other starting times by choosing appropriate starting values for V and q. The ODE of the expected quadratic variation of dV_t can be derived directly from its SDE as

$$\mathbb{E}_0^{\mathbb{Q}}(dV_t)^2 = [\sigma_V^2 \mathbb{E}_0^{\mathbb{Q}} q_t + 2\mu_V^2 \lambda_1^V \mathbb{E}_0^{\mathbb{Q}} V_t]dt,$$

since $\mathbb{E}_0^{\mathbb{Q}} Z_V^2 = 2\mu_V^2$ and $(dN_t)^2 = dN_t$. The SDE of V_t^2 can be written by using Itô as

$$\begin{aligned} dV_t^2 &= 2V_t dV_t + (dV_t)^2 + (2V_t Z_V + Z_V^2)dN_t \\ &= [2V_t\kappa_V(\bar{V} - V_t) + \sigma_V^2 q_t]dt + \sigma_V V_t \sqrt{q_t} dW_t^V + (2V_t Z_V + Z_V^2)dN_t. \end{aligned} \tag{A.9}$$

This yields

$$(dV_t^2)^2 = \sigma_V V_t^2 q_t dt + (4V_t^2 Z_V^2 + 4V_t Z_V^3 + Z_V^4)dN_t,$$

which leads to the following ODE

$$\begin{aligned}\mathbb{E}_0^{\mathbb{Q}}(dV_t^2)^2 = [&\sigma_V \mathbb{E}_0^{\mathbb{Q}} V_t^2 q_t dt + 24\mu_V^3 \lambda_1^V d\mathbb{E}_0^{\mathbb{Q}} V_t^2 + 24\mu_V^4 \lambda_1^V d\mathbb{E}_0^{\mathbb{Q}} V_t \\ &+ 8\mu_V^2 \lambda_1^V d\mathbb{E}_0^{\mathbb{Q}} V_t + 8\mu_V^2 \lambda_1^V \mathbb{E}_0^{\mathbb{Q}} V_t^3]dt.\end{aligned}$$

In addition, (A.9) in combination with the SDE of V_t yields the ODE

$$\mathbb{E}_0^{\mathbb{Q}}(dV_t dV_t^2) = [2\sigma_V \mathbb{E}_0^{\mathbb{Q}} V_t q_t + 4\mu_V \lambda_1^V \mathbb{E}_0^{\mathbb{Q}} V_t^2 + 6\mu_V \lambda_1^V \mathbb{E}_0^{\mathbb{Q}} V_t]dt.$$

Further

$$\begin{aligned}\mathbb{E}_0^{\mathbb{Q}}(dq_t)^2 &= \sigma_q^2 \mathbb{E}_0^{\mathbb{Q}} q_t dt, \\ \mathbb{E}_0^{\mathbb{Q}} dq_t dV_t &= \rho\sigma_q\sigma_V \mathbb{E}_0^{\mathbb{Q}} q_t dt\end{aligned}$$

and

$$\mathbb{E}_0^{\mathbb{Q}} dq_t dV_t^2 = 2\rho\sigma_q\sigma_V \mathbb{E}_0^{\mathbb{Q}} V_t q_t dt.$$

To solve the ODEs in closed form we have to compute the higher moments of V and q. This can be done iteratively by starting to solve the ODEs for the first moments, using Itô in combination with the *variation of constants* method. It holds

$$\begin{aligned}\frac{d\mathbb{E}_0^{\mathbb{Q}} dV_t}{dt} &= \mathbb{E}_0^{\mathbb{Q}} \kappa_V(\bar{V} - V_t) + \mu_V \lambda_1^V \mathbb{E}_0^{\mathbb{Q}} V_t \\ &= \underbrace{(\mu_V \lambda_1^V - \kappa_V)}_{\equiv a_V} \mathbb{E}_0^{\mathbb{Q}} V_t + \underbrace{\kappa_V \bar{V}}_{\equiv \alpha_V},\end{aligned}$$

and hence

$$\begin{aligned}\mathbb{E}_0^{\mathbb{Q}} V_t &= V_0 e^{a_V t} + e^{a_V t} \int_0^t e^{-a_V s} \alpha_V ds \\ &= V_0 e^{a_V t} + \alpha_V \frac{e^{a_V t} - 1}{a_V}.\end{aligned}$$

Similarly it follows

$$\begin{aligned}\mathbb{E}_0^{\mathbb{Q}} q_t &= q_0 e^{-\kappa_q t} + e^{-\kappa_q t} \int_0^t e^{\kappa_q s} \kappa_q \bar{q} ds. \\ &= q_0 e^{-\kappa_q t} + \kappa_q \bar{q} \frac{e^{-\kappa_q t} - 1}{-\kappa_q}.\end{aligned}$$

From the SDE of V_t^2 we get

$$\frac{d\mathbb{E}_0^{\mathbb{Q}} dV_t^2}{dt} = \underbrace{-2\kappa_V + 2\mu_V \lambda_1^V}_{\equiv a_{V^2}} \mathbb{E}_0^{\mathbb{Q}} V_t^2 + \underbrace{(2\kappa_V \bar{V} + 2\mu_V \lambda_1^V)}_{\equiv \varphi_{V^2:V}} \mathbb{E}_0^{\mathbb{Q}} V_t + \underbrace{\sigma_V^2}_{\equiv \varphi_{V^2:q}} \mathbb{E}_0^{\mathbb{Q}} q_t,$$

hence

$$\mathbb{E}_0^{\mathbb{Q}} V_t^2 = V_0^2 e^{a_{V^2} t} + e^{a_{V^2} t} \int_0^t e^{-a_{V^2} s} (\varphi_{V^2:V} \mathbb{E}_0^{\mathbb{Q}} V_s + \varphi_{V^2:q} \mathbb{E}_0^{\mathbb{Q}} q_s) ds,$$

where we can solve the integrals analytically by plugging in the solutions for the lower moments. To calculate the expected value of q_t^2 we note

$$\frac{d\mathbb{E}_0^{\mathbb{Q}} dq_t^2}{dt} = \underbrace{-2\kappa_q}_{\equiv a_{qq}} \mathbb{E}_0^{\mathbb{Q}} q_t^2 + \underbrace{(2\kappa_q \bar{q} + \sigma_q^2)}_{\equiv \varphi_{q^2:q}} \mathbb{E}_0^{\mathbb{Q}} q_t,$$

which gives

$$\mathbb{E}_0^{\mathbb{Q}} q_t^2 = q_0^2 e^{a_{qq}t} + e^{a_{qq}t} \int_0^t e^{-a_{qq}s} (\varphi_{q^2:q} \mathbb{E}_0^{\mathbb{Q}} q_s) ds.$$

Using the product rule for semi-martingales for the cross-moment $\mathbb{E}_0^{\mathbb{Q}} V_t q_t$ it holds that

$$dV_t q_t = V_t \kappa_q (\bar{q} - q_t) dt + q_t \kappa_V (\bar{V} - V_t) dt + q_t Z_V dN_t + \rho_{Vq} \sigma_V \sigma_q q_t dt + [\text{Diffusion Terms}]_t.$$

This leads to

$$\frac{d\mathbb{E}_0^{\mathbb{Q}} dV_t q_t}{dt} = \underbrace{\left(-\kappa_q - \kappa_V + \mu_V \lambda_1^V\right)}_{\equiv a_{Vq}} \mathbb{E}_0^{\mathbb{Q}} V_t q_t + \underbrace{\kappa_q \bar{q}}_{\equiv \varphi_{Vq:V}} \mathbb{E}_0^{\mathbb{Q}} V_t + \underbrace{\left(\kappa_V \bar{V} + \rho \sigma_V \sigma_q\right)}_{\equiv \varphi_{Vq:q}} \mathbb{E}_0^{\mathbb{Q}} q_t,$$

hence

$$\mathbb{E}_0^{\mathbb{Q}} V_t q_t = V_0 q_0 e^{a_{Vq}t} + e^{a_{Vq}t} \int_0^t e^{-a_{Vq}s} (\varphi_{Vq:V} \mathbb{E}_0^{\mathbb{Q}} V_s + \varphi_{Vq:q} \mathbb{E}_0^{\mathbb{Q}} q_s) ds.$$

Using Itôm we first derive for the expectation of V_t^3

$$dV_t^3 = 3V_t(\kappa_V(\bar{V} - V_t)dt + \sigma_V \sqrt{q_t} dW_t^V) + 3\sigma_V^3 V_t q_t dt + (3V_t^2 Z_V + 3V_t + Z_V^2 + Z_V^3) dN_t,$$

hence

$$\begin{aligned} \frac{d\mathbb{E}_0^{\mathbb{Q}} dV_t^3}{dt} = & \underbrace{\left(-3\kappa_V + 3\mu_V \lambda_1^V\right)}_{\equiv a_{V^3}} \mathbb{E}_0^{\mathbb{Q}} V_t^3 + \underbrace{\left(3\kappa_V \bar{V} + 3\sigma_V^2 + 6\mu_V^2 \lambda_1^V\right)}_{\equiv \varphi_{V^3:V^2}} \mathbb{E}_0^{\mathbb{Q}} V_t^2 \\ & + \underbrace{6\lambda_1^V \mu_V^3}_{\equiv \varphi_{V^3:V}} \mathbb{E}_0^{\mathbb{Q}} V_t \end{aligned}$$

and therefore

$$\mathbb{E}_0^{\mathbb{Q}} V_t^3 = V_0^3 e^{a_{V^3}t} + e^{-a_{V^3}t} \int_0^t e^{-a_{V^3}s} (\varphi_{V^3:V^2} \mathbb{E}_0^{\mathbb{Q}} V_s^2 + \varphi_{V^3:V} \mathbb{E}_0^{\mathbb{Q}} V_s) ds.$$

For the cross moment $\mathbb{E}_0^{\mathbb{Q}} V_t^2 q_t$ we derive the following SDE first by using the results for V_t^2 and the product rule

$$\begin{aligned} dV_t^2 q_t = & q_t(2V_t \kappa_V (\bar{V} - V_t) dt + 2\sigma_V V_t \sqrt{q_t} dW_t^V + \sigma_V^2 q_t dt) \\ & + V_t^2 (\kappa_q (\bar{q} - q_t) dt + \sigma_q \sqrt{q_t} dW_t^q) \\ & + 2\rho_{vq} \sigma_V \sigma_q V_t q_t dt \\ & + (2V_t q_t Z_V + q_t Z_V^2) dN_t^V. \end{aligned}$$

Thus

$$\frac{d\mathbb{E}_0^{\mathbb{Q}} dV^2 q_t}{dt} = \underbrace{(-\kappa_q - 2\kappa_V + 4\mu_V \lambda_1^V)}_{\equiv a_{V^2 q}} \mathbb{E}_0^{\mathbb{Q}} V_t^2 q_t + \underbrace{\kappa_q \bar{q}}_{\equiv \varphi_{V^2 q:V^2}} \mathbb{E}_0^{\mathbb{Q}} V_t^2 + \underbrace{\sigma_V^2}_{\equiv \varphi_{V^2 q:q^2}} \mathbb{E}_0^{\mathbb{Q}} q_t^2 + \underbrace{(2\kappa_V \bar{V} + 4\mu_V^2 \lambda_1^V + 2\rho_{vq}\sigma_V \sigma_q)}_{\equiv \varphi_{V^2 q:Vq}} \mathbb{E}_0^{\mathbb{Q}} V_t q_t,$$

which induces

$$\mathbb{E}_0^{\mathbb{Q}} V_t^2 q_t = V_0^2 q_0 e^{a_{V^2 q} t} + e^{a_{V^2 q} t} \int_0^t e^{-a_{V^2 q} s} (\varphi_{V^2 q:V^2} \mathbb{E}_0^{\mathbb{Q}} V_s^2 + \varphi_{V^2 q:q^2} \mathbb{E}_0^{\mathbb{Q}} q_s^2 + \varphi_{V^2 q:Vq} \mathbb{E}_0^{\mathbb{Q}} V_s q_s) ds.$$

Now, by iteration every moment can be calculated in closed form. Afterwards, the same can be done for the integrals of the quadratic variation of the futures price in (A.8).

A.3 Calibration of the VVIX Approximation

To estimate a proper parameter set $\{a_0, y\}$ for the VVIX_t^τ approximation in (A.2) for a certain day t, we choose to calibrate the dynamics of the approximated VIX given by $(f_{a_0,y}(A^{\text{VIX}} + B^{\text{VIX}\prime} Y_{t+s}))_s$ to the dynamics of the model-implied VIX given by Equation (14) over the time interval 0 to T. The idea is that the VIX index dynamics proxy the VIX futures dynamics and if the approximated VIX dynamics equals those of the model-implied VIX, the induced dynamics of the approximated VIX futures should be close to the model's VIX futures dynamics. As a result, the approximated VVIX, which is essentially the quadratic variation of the approximated futures price, should closely match the exact VVIX.

During the calibration we estimate the parameter set $\{a_0, y\}$ in a two step procedure. In the first step we simulate for date t the VIX up to time $t+T$ using its known representation from Equation (14) and then minimize the expected squared difference in variation by solving

$$\underset{\{y_1,y_2\}}{\arg\min}\, \mathbb{E}_t \int_0^T \Big(\int_0^t (df_{1,y}(A^{\text{VIX}} + B^{\text{VIX}\prime} Y_u))^2 - (d\text{VIX}_u)^2 \, du \Big)^2, \tag{A.10}$$

where we assume $y_0, a_0 = 1$.[46] Since y_0 cannot be identified by this procedure we minimize in a second step the expected level difference

$$\underset{y_0}{\arg\min}\, \mathbb{E}_t \int_0^T (f_{1,y}(A^{\text{VIX}} + B^{\text{VIX}\prime} Y_s) - \text{VIX}_s)^2. \tag{A.11}$$

[46] This is no limitation since y_0 only effects the level of the approximation. Furthermore, the influence of a_0 can be offset by the y_i's.

In Section 3.3.2 we show that the approximation works quite accurate, which may seem quite surprising on first glance because the calibration procedure only takes the first two moments into account. In appendix A.4 we explain the mathematical intuition of our calibration approach, which bases on a theorem on stochastic processes. There, we also try to shed some light on the resulting performance of our approximation. In the subsequent chapter, we show further that our approach yields not only a sufficient good result for the approximated VIX, but also for VVIX term structure.

A.4 Mathematical Foundation of our Calibration Procedure from Appendix A.3

For notational ease define for a process X_t its quadratic variation as $\langle X_\bullet \rangle_t \equiv \int_0^t (dX_s)^2 ds$. The following theorem was first proven by Rebolledo (1980) in more generality and under some assumptions which are satisfied in our setting.

Theorem 1 (Functional Central Limit Theorem for Local Martingales) *Suppose for each $n \geq 0$, $M^{(n)}$ are local martingales on $[0,T]$ and $M = M_0 + \int \sigma dW_t$ for some $\sigma \geq 0$ and Wiener-Process W such that*

$$\lim_{n\to\infty} \mathbb{E}[\sup_{0\leq s\leq T} (\langle M_\bullet^{(n)} \rangle_s - \langle M_\bullet^{(n)} \rangle_{s-})^2] = 0,$$

$$\lim_{n\to\infty} \mathbb{E}[\sup_{0\leq s\leq T} (\langle M_\bullet^{(n)} \rangle_s - \langle M_\bullet \rangle_s)^2] = 0 \tag{A.12}$$

and

$$\lim_{n\to\infty} \mathbb{E}[\sup_{0\leq s\leq T} (M_s^{(n)} - M_s)^2] = 0. \tag{A.13}$$

Then it holds

$$M^{(n)} \underset{n\to\infty}{\to}^{d} M,$$

where $\underset{n\to\infty}{\to}^{d}$ indicates convergence in distribution. Therefore the limit distribution of $M^{(n)}$ equals the one of M.

The interpretation of the theorem is as follows: If the variation of the approximated process $M^{(n)}$ and its mean is sufficient close to the real process M over the whole time interval, the distributional behavior and hence its overall dynamics is very close to the real one as well. The theorem's requirements (A.12) and (A.13) are directly targeted by the first (A.10) and second (A.11) step of our calibration procedure if we set $M^{(n)} = f_{a_0,y}(A^{\text{VIX}} + B^{\text{VIX}\prime} Y)$ and $M = \text{VIX}^{30\text{D}}$. Considering the above very strong result for a diffusive setting, it is not surprising that numerical results support the validity of our method in a jump diffusion environment and leads to small errors for the moments even above second order as documented in Table 9.

A.5 Implementation of our Calibration Procedure from Section A.3

For the calibration we first simulate the state variables M times from time t to time $t+T$. For the first step we minimize the squared difference of the expected variation paths

$$\arg\min_{y_1,y_2} \frac{1}{M}\sum_{k=1}^{M}\sum_{i=2}^{N}\Big(\sum_{j=1}^{i-1}(\Delta f_{1,y}(A^{\text{VIX}}+B^{\text{VIX}\prime}V_{t_j}^{(k)}))^2-(\Delta\text{VIX}(V_{t_j}^{(k)}))^2\Big)^2,$$

where $0=t_1<\cdots<t_N=T$, $\Delta X_l\equiv X_{l+1}-X_l$ and $V_{t_j}^{(k)}$ is the simulated volatility at time t_j in k-th simulation. The model's state variables are simulated efficiently using advanced simulation schemes: To simulate q_t we use the QE algorithm proposed in Andersen (2008) and for the discretization of V_t we use a modification of the scheme proposed by Broadie and Kaya (2006). We find that such advanced simulation schemes are necessary to simulate the model with desired accuracy, especially the higher moments of the state variables.
For the second step we minimize the squared difference of the expected paths

$$\arg\min_{y_0} \frac{1}{M}\sum_{k=1}^{M}\sum_{i=1}^{N}\Big(f_{a_0,y}(A^{\text{VIX}}+B^{\text{VIX}}V_{t_i}^{(k)})-\text{VIX}(V_{t_i}^{(k)})\Big)^2,$$

to estimate y_0.

A.6 Simulation of the VVIX Term Structure and Calculation of the Relative Error $\epsilon^{\tau}_{\text{VVIX}}$

For each day t of our sample we simulate the model from Section 3.1 for $T=5$ months starting from the respective state variables q_t and V_t. Afterwards we calibrate the approximated VIX futures dynamics using the minimization procedure described in Appendix (A.3). Then we simulate the exact VVIX_t^{τ} term structure for $\tau=1,2,3,4,5$ months as given in (12) using Monte Carlo simulation techniques which rely on the result from Barndorff-Nielsen and Shephard (2004)

$$\mathbb{E}_t^{\mathbb{Q}}\int_t^{t+T}(dX_s)^2ds=\mathbb{E}_t^{\mathbb{Q}}\lim_{N\to\infty}\sum_{j=1}^{N}(X_{t_i}-X_{t_{i+1}})^2,$$

for $t\le t_i\le t+T$ and $\lim_{N\to\infty}|t_i-t_{i+1}|=0$. Therefore, the exact VVIX term structure can be simulated as

$$\Big(\text{VVIX}_t^{\tau}\Big)^2=\frac{1}{M}\sum_{k=1}^{M}\sum_{i=1}^{N}(\ln \text{F}_{t_i,X_{t_i}^k}^{t+\tau}-\ln \text{F}_{t_{i+1},X_{t_{i+1}}^k}^{t+\tau})^2, \tag{A.14}$$

where M is the number of simulated model paths, $X_{t_i}^k$ the vector of state variables for the k-th path at time t_i and $\mathrm{F}_{t_i,X_{t_i}^k}^{t+\tau}$ is the VIX futures price at time t_i and maturity in $t+\tau$ with respect to the state $X_{t_i}^k$. The futures price is calculated using Fourier transformation methods which rely on techniques explained in Chen and Joslin (2012) and Duffie, Pan, and Singleton (2000). Details can be found in the appendix of Branger, Kraftschik, and Völkert (2016). To calculate the log approximation (A.6) we simulate in addition

$$\left(\mathrm{RV}_t^{\mathrm{Fut},\tau}\right)^2 = \frac{1}{M}\sum_{k=1}^{M}\sum_{i=1}^{N}(\mathrm{F}_{t_i,X_{t_i}^k}^{t+\tau} - \mathrm{F}_{t_{i+1},X_{t_{i+1}}^k}^{t+\tau})^2, \tag{A.15}$$

and estimate $\widehat{\frac{1}{(\mathrm{F}_t^{t+\tau})^2}}$ as the ratio of (A.14) and (A.15).

A.7 Reasoning the Time-Varying Property of A^{VVIX}

The higher-order approximation for the VVIX in dependence of the state vector $\widetilde{Y}_t = [V^3, V^2q, V^2, q^2, Vq, V, q]'$, which we use throughout the paper is

$$(\mathrm{VVIX}_t^\tau)^2 \approx A^{\mathrm{VVIX}}(\Theta,\tau,y_t) + \ B^{\mathrm{VVIX}}(\Theta,\tau,y_t)'\widetilde{Y}_t.$$

Thus, the intercept $A^{\mathrm{VVIX}}(\Theta,\tau,y_t)$ is time depending and not constant. This finding can be reasoned by an alternative and more simple approximation, which we conduct in the following. In what follows we denote the log-approximation by c. It holds

$$\begin{aligned}
(\mathrm{VVIX}_t^\tau)^2 &= \frac{1}{\tau}\left[\mathbb{E}_t\int_0^\tau \left(d\ln \mathrm{F}_s^{t+\tau}\right)^2\right] \\
&= \frac{c}{\tau}\mathbb{E}_t\left[\int_0^\tau \left(d\mathbb{E}_s\left[\mathrm{VIX}_{t+\tau}^{30\mathrm{D}}\right]\right)^2\right] \\
&= \frac{c}{\tau}\mathbb{E}_t\left[\int_0^\tau \left(d\mathbb{E}_s\left[\sqrt{A^{\mathrm{VIX}}+B^{\mathrm{VIX}}V_{t+\tau}}\right]\right)^2\right] \\
&\approx \frac{c}{\tau}\mathbb{E}_t\left[\int_0^\tau \left(d\mathbb{E}_s\left[\frac{B^{\mathrm{VIX}}}{2\sqrt{A^{\mathrm{VIX}}+B^{\mathrm{VIX}}V_t}}V_{t+\tau}\right]\right)^2\right],
\end{aligned}$$

where we use a first-order Taylor approximation for the square root around V_t. Thus, further simplifications yield

$$\begin{aligned}
(\mathrm{VVIX}_t^\tau)^2 &= \frac{c}{4\tau}\frac{B^{\mathrm{VIX}}}{A^{\mathrm{VIX}}+B^{\mathrm{VIX}}V_t}\mathbb{E}_t\left[\int_0^\tau \sigma_V^2\left[\beta_q^q(\tau(s))q_s + \alpha^q(\tau(s))\right]ds\right] \\
&= \frac{c}{4\tau}\frac{B^{\mathrm{VIX}}\sigma_V^2\left(B_q^q(\tau)q_t + A_q^q(\tau)\right)}{A^{\mathrm{VIX}}+B^{\mathrm{VIX}}V_t}, \\
&\equiv \frac{\gamma q_t+\eta}{A^{\mathrm{VIX}}+B^{\mathrm{VIX}}V_t},
\end{aligned} \tag{A.16}$$

where we use $\mathbb{E}_t\left[\int_0^\tau \beta_q^q(\tau(s))q_s + \alpha^q(\tau(s))ds\right] = B_q^q(\tau)q_t + A_q^q(\tau)$ for which we provide a proof in Appendix A.2. In addition, since both approximation methods cannot be mapped onto each other directly by simple mathematical manipulations, we regress

$$A^{\text{VVIX}}(\Theta, \tau, y_t) = \alpha + \gamma \frac{q_t}{A^{\text{VIX}} + B^{\text{VIX}} V_t} + \eta \frac{1}{A^{\text{VIX}} + B^{\text{VIX}} V_t} + \epsilon_t.$$

The regression yields an average adj. R^2 of 99.5% across all maturities τ and highly significant, positive estimates for γ and η, as predicted by Equation (A.16). Therefore, the intercept $A^{\text{VVIX}}(\Theta, \tau, y_t)$ corresponds to the resulting VVIX approximation if we would approximate the square root by a first order Taylor series and would forgo higher dimensions. More importantly, the regression results indicate that our higher order approximation from Equation (15) basically adds correction terms to the above (most simple) approximation. These higher order terms are especially important during market turmoil, e.g. high VVIX and VIX values. During these times, $A^{\text{VVIX}}(\Theta, \tau, y_t)$ takes very low values and the main risk contribution to the VVIX term structure stems mainly from jump risk as well as continuous vol-of-vol risk (q) and not from the intercept, as we show in Section 4.1.

References

Ait-Sahalia, Y., M. Karaman, and L. Mancini, 2015, The Term-Structure of Variance Swaps and Risk Premia, *Journal of Financial Economics* forthcoming.

Amengual, D., 2008, The Term Structure of Variance Risk Premia, *Working Paper*.

Andersen, L., 2008, Efficient Simulation of the Heston Stochastic Volatility Model, *Journal of Computational Finance* 11, 1–42.

Andersen, L., and V. Piterbarg, 2007, Moment explosions in stochastic volatility models, *Finance and Stochastics* 11, 29–50.

Andersen, Torben G., Nicola Fusari, and Viktor Todorov, 2015, Parametric Inference and Dynamic State Recovery From Option Panels, *Econometrica* 83, 1081–1145.

Bakshi, G., N. Kapadia, and D. Madan, 2003, Stock Return Characteristics, Skew Laws, and Differential Pricing of Individual Equity Options, *Review of Financial Studies* 16, 101–143.

Bardgett, C., E. Gourier, and M. Leippold, 2016, Inferring volatility dynamics and risk premia from the S&P500 and VIX markets, Swiss Finance Institute Research Paper No. 13-40.

Barndorff-Nielsen, O., and N. Shephard, 2004, Power and Bipower Variation with Stochastic Volatility and Jumps, *Journal of Financial Econometrics* 2, 1–37.

Bates, D., 2000, Post-'87 Crash Fears in the S&P Futures Option Market, *Journal of Econometrics* 94, 181–238.

Bates, D., 2006, Maximum Likelihood Estimation of Latent Affine Processes, *Review of Financial Studies* 19, 909–965.

Billingsley, P., 1968, Convergence of probability measures, *Wiley*.

Bollerslev, T., G. Tauchen, and H. Zhou, 2009, Expected Stock Returns and Variance Risk Premia, *Review of Financial Studies* 22, 4463–4492.

Branger, N., A. Kraftschik, and C. Völkert, 2016, The Fine Structure of Variance: Consistent Pricing VIX Derivatives in Consistent and Log-VIX Models, Working Paper.

Brenner, M., E.Y. Ou, and J.E. Zhang, 2006, Hedging volatility risk, *Journal of Banking & Finance* 30, 811–821.

Britten-Jones, M., and A. Neuberger, 2000, Option Prices, Implied Price Processes, and Stochastic Volatility, *Journal of Finance* 55, 839–866.

Broadie, M., and Ö. Kaya, 2006, Exact Simulation of Stochastic Volatility and Other Affine Jump Diffusion Processes, *Operations Research* 54, 217–231.

Brockhaus, O., and Long D., 2000, Volatility swaps made simple, *Risk* 13, 13–29.

Buraschi, A., F. Trojani, and A. Vedolin, 2008, The Joint Behavior of Credit Spreads, Stock Options and Equity Returns When Investors Disagree, Working Paper.

Carr, P., and D. Madan, 1998, Towards a Theory of Volatility Trading, in R. Jarrow, eds.: *Volatility: New Estimation Techniques for Pricing Derivatives* (Risk Publications,).

Carr, P., and L. Wu, 2009, Variance Risk Premiums, *Review of Financial Studies* 22, 1311–1341.

CBOE, 2009, The CBOE Volatility Index – VIX, White Paper.

Chen, H., and S. Joslin, 2012, Generalized Transform Analysis of Affine Processes and Applications in Finance, *Review of Financial Studies* 25, 2225–2256.

Christoffersen, P., S. Heston, and K. Jacobs, 2009, The Shape and Term Structure of the Index Option Smirk: Why Multifactor Stochastic Volatility Models Work so Well, *Management Science* 55, 1914–1932.

Cochrane, J., and M. Piazzesi, 2005, Bond Risk Premia, *American Economic Review* 94(1), 138–160.

Coval, J. D., and T. Shumway, 2001, Expected Option Returns, *Journal of Finance* 56, 983–1009.

Daal, E., A. Naka, and J. Yu, 2007, Volatility clustering, leverage effects, and jump dynamics in the US and emerging Asian equity markets, *Journal of Banking & Finance* 31, 2751–2769.

Demeterfi, K., E. Derman, M. Kamal, and J. Zou, 1999, A Guide to Volatility and Variance Swaps, *Journal of Derivatives* 4, 9–32.

Duffie, D., J. Pan, and K. Singleton, 2000, Transform Analysis and Asset Pricing for Affine Jump-Diffusions, *Econometrica* 68, 1343–1376.

Eraker, B., M. Johannes, and N. Polson, 2003, The Impact of Jumps in Volatility and Returns, *Journal of Finance* 58, 1269–1300.

Fan, R., A. Gupta, and P. Ritchken, 2003, Hedging in the Possible Presence of Unspanned Stochastic Volatility: Evidence from Swaption Markets, *Journal of Finance* 58, 2219–2248.

Fowler, D., and E. Robson, 1998, Square Root Approximations in Old Babylonian Mathematics, *Historia Mathematica* 25, 366–378.

Hollstein, Fabian, and Marcel Prokopczuk, 2017, How Aggregate Volatility-of-Volatility Affects Stock Returns, *Review of Asset Pricing Studies (forthcoming)*.

Huang, D., and I. Shaliastovich, 2014, Volatility-of-Volatility Risk, *Working Paper*.

Huang, J., and L. Wu, 2004, Specification Analysis of Option Pricing Models Based on Time-Changed Levy Processes, *Journal of Finance* 59, 1405–1439.

Huskaj, B., and M. Nossman, 2013, A Term Structure Model for VIX Futures, *Journal of Futures Markets* 33, 421–442.

Jiang, G., and Y. Tian, 2005, The Model-Free Implied Volatility and Its Information Content, *Review of Financial Studies* 18, 1305–1342.

Jiang, G., and Y. Tian, 2007, Extracting Model-Free Volatility from Option Prices: An Examination of the VIX Index, *Journal of Derivatives* 14, 1–26.

Johnson, L., 2016, Risk Premia and the VIX Term Structure, *Journal of Financial Quantitative Analysis (forthcoming)*.

Kaeck, Andreas, 2017, Variance-of-variance risk premium, *Review of Finance* p. rfx008.

Lin, Y., 2007, Pricing VIX Futures: Evidence from Integrated Physical and Risk Neutral Probability Measures, *Journal of Futures Markets* 27, 1175–1217.

Luo, X., and J. E. Zhang, 2012, The Term Structure of VIX, *Journal of Futures Markets* 32, 1092–1123.

Luo, Z., and Y. Zhu, 2010, Volatility Components: The Term Strutcture Dynamics of VIX Futures, *Journal of Futures Markets* 30, 230–256.

Mencia, J., and E. Sentana, 2013, Valuation of VIX Derivatives, *Journal of Financial Economics* 108, 367–391.

Ni, S.X., J. Pan, and A.M. Poteshman, 2008, Volatility Information Trading in the Option Market, *Journal of Finance* 63, 1059–1091.

Park, Yang-Ho, 2015, Volatility-of-Volatility and tail risk hedging returns, *Journal of Financial Markets* 26, 38–63.

Rebolledo, R., 1980, Central Limit Theorems for Local Martingales, *Probability Theory and Related Fields* 51, 269–286.

Sepp, A., 2008a, Pricing Options on Realized Variance in Heston Model with Jumps in Returns and Volatility, *Journal of Computational Finance* 11, 33–70.

Sepp, A., 2008b, VIX Option Pricing in a Jump-Diffusion Model, *Risk* 21, 84–89.

Wang, Y., C. Zixing, and Q. Zhang, 2011, Differential Evolution with Composite Trial Vector Generation Strategies and Control Parameters, *Evolutionary Computation, IEEE Transaction on* 15(1), 55–66.

Zang, Xin, Jun Ni, Jing-Zhi Huang, and Lan Wu, 2017, Double-Jump Diffusion Model for VIX: Evidence from VVIX, *Quantitative Finance* 17, 227–240.

Descriptives of the Daily VVIX Term Structure					
Maturity	30	60	90	120	150
Mean	84.76	74.14	66.75	61.42	57.57
Median	83.21	74.27	67.01	61.6	57.79
Min	57.56	52.24	46.99	45.41	40.85
Max	145.44	105.23	90.88	83.33	78.27
Std.	12.92	9.43	7.89	6.77	5.84
Skewness	0.78	0.23	-0.03	-0.11	-0.24
Kurtosis	4.05	2.75	2.5	2.61	2.76
AC(1)	0.9357	0.9715	0.9827	0.9858	0.9856
Corr($\ln \Delta \text{VVIX}^{\tau}$)	1	0.85	0.74	0.67	0.55
		1	0.86	0.76	0.63
			1	0.85	0.69
				1	0.77
					1
Corr($\ln \Delta \text{VVIX}^{\tau}$, $\ln \Delta$S&P500)	-0.5295	-0.5285	-0.5138	-0.4816	-0.3937
Corr($\ln \Delta \text{VVIX}^{\tau}$, $\ln \Delta \text{VIX}^{30D}$)	0.45	0.41	0.40	0.38	0.36
...	0.46	0.45	0.42	0.42	0.39
...	0.43	0.44	0.41	0.40	0.37
...	0.40	0.42	0.39	0.38	0.35
Corr($\ln \Delta \text{VVIX}^{\tau}$, $\ln \Delta \text{VIX}^{150D}$)	0.40	0.42	0.37	0.38	0.36

Table 1: The table shows descriptives of the VVIX term structure for 30 to 150 days. The sample period is from 09/01/2007 to 08/31/2014. We discard days which would require an extrapolation above 150 days of maturity.

Principle Component Analysis					
	"Level"	*"Slope"*			
	PC1	PC2	PC3	PC4	PC5
$\text{VVIX}^{30\text{D}}$	0.42	0.75	0.45	-0.23	0.08
$\text{VVIX}^{60\text{D}}$	0.46	0.27	-0.52	0.59	-0.32
$\text{VVIX}^{90\text{D}}$	0.46	-0.15	-0.47	-0.36	0.64
$\text{VVIX}^{120\text{D}}$	0.45	-0.36	0.05	-0.49	-0.65
$\text{VVIX}^{150\text{D}}$	0.45	-0.46	0.55	0.48	0.25
% of var.	91.99	6.50	1.15	0.27	0.10

Table 2: The table shows the coefficients defining each principle component of the VVIX term structure from 09/01/2007 to 08/31/2014 and gives the percentage of the term structure's variance, explained by each principle component.

Descriptives of Daily S&P500 Excess Straddle Returns						
Mat. in Month	1	2	3	6	9	12
Mean	-0.0050***	-0.0027***	-0.0017***	-0.0008*	-0.0004	-0.0002
Median	-0.0165***	-0.0075***	-0.0049***	-0.0025***	-0.0017***	-0.0012***
Standard dev.	0.0631	0.0347	0.0262	0.0172	0.0139	0.0123
Skewness	2.1789	1.8384	1.6529	1.3299	1.0784	1.0071
Kurtosis	11.3973	10.2178	9.7731	8.7196	7.5532	7.4879

Descriptives of Daily VIX Straddle Excess Returns					
Mat. in Month	1	2	3	4	5
Mean	-0.0037***	-0.0014	-0.0003	-0.0005	-0.0007
Median	-0.0189***	-0.0073***	-0.0046***	-0.0031***	-0.0027***
Standard dev.	0.0774	0.0366	0.0275	0.0227	0.0196
Skewness	6.1137	1.3043	2.1203	1.1821	1.4392
Kurtosis	89.0006	17.4381	18.8963	12.2675	12.6745

Table 3: The table shows descriptives for daily S&P500 and VIX straddle returns from 09/01/2007 to 08/31/2014. *,** and *** indicate statistical significance at the 90, 95, and 99% confidence level.

Correlations of different variance risk measures					
	$VVIX^{30D}$	$Slope^{VVIX}$	VIX^{30D}	$Slope^{VIX}$	VRP
Mean	84.7446	0.0000	22.0885	0.0000	0.0227
Median	83.2143	-0.0844	19.1540	0.0205	0.0178
Std.	12.9183	0.5965	10.4155	0.3636	0.0288
Skewness	0.7795	0.6891	2.0613	-3.6213	-0.0993
Kurtosis	4.0458	3.5675	8.2700	26.2873	31.3218
$VVIX^{30D}$	1				
$Slope^{VVIX}$	0.4330	1			
VIX^{30D}	0.4246	0.3389	1		
$Slope^{VIX}$	-0.1392	-0.2317	-0.1823	1	
VRP	0.1727	0.1158	0.4273	0.2429	1

Table 4: The table shows correlations for our different risk measures. Correlations of the $VVIX^{30D}$, $Slope^{VVIX}$, VIX^{30D}, $Slope^{VIX}$ and VRP are calculated using daily data from 09/01/2007 to 08/31/2014.

Multivariate Regressions for Daily VIX Straddle Excess Returns					
Maturity	1	2	3	4	5
Intercept	0.0093 (0.6463)	0.0055 (0.8553)	0.0040 (0.7549)	0.0024 (0.4909)	−0.0007 (−0.134)
VVIX^{30D}	−0.0015 (−0.6538)	−0.0010 (−0.9749)	−0.0007 (−0.8698)	−0.0004 (−0.4721)	0.0002 (0.2377)
$\text{Slope}^{\text{VVIX}}$	0.0004 (0.1820)	0.0042^{***} (4.0745)	0.0040^{***} (4.7742)	0.0032^{***} (3.9569)	0.0031^{***} (3.3867)
$\text{Slope}^{\text{VIX}}$	−0.0013 (−0.6061)	0.0014 (1.3822)	0.0002 (0.2739)	−0.0002 (−0.3188)	0.0000 (−0.0138)
VIX^{30D}	−0.0007 (−0.2674)	0.0010 (0.9356)	0.0014 (1.4401)	0.0016 (1.4872)	0.0015 (1.1097)
VRP	−0.0020 (−0.878)	-0.0033^{***} (−3.0819)	-0.0030^{***} (−3.2245)	-0.0043^{***} (−5.0307)	-0.0057^{***} (−4.0646)
$\text{r}_t^{\text{Straddle}}$	−0.0025 (−1.2315)	-0.0033^{***} (−3.5293)	-0.0017^{**} (−2.2274)	0.0010 (1.4474)	0.0003 (0.4239)
adj. R^2	-0.0003	0.0177	0.0225	0.0420	0.0258

Table 5: Regression: $\text{r}_{t+1}^{\text{Straddle}} = \alpha + \beta_1' X_t + \beta_2 \text{r}_t^{\text{Straddle}} + \epsilon_{t+1}$, where $\text{r}_{t+1}^{\text{Straddle}}$ is the daily excess return of a straddle on the VIX with maturities of $1, 2, 3, 4$ and 5 months from end of day t to end of day $t+1$. X_t is a standardized vector of explanatory variables observed at the end of day t. VVIX^{30D} is the implied volatility-of-volatility index, $\text{Slope}^{\text{VVIX}}$ is the second PCA component of the VVIX term structure, $\text{Slope}^{\text{VIX}}$ is the second PCA component of the VIX term structure, VIX^{30D} is the volatility index and the variance risk premium (VRP) is calculated as the differential of the risk-neutral and the physical expectation of the variation of the stock index over the next 30 days. For the regressions we use daily data samples from 09/01/2007 to 08/31/2014. *,** and *** indicate statistical significance at the 90, 95, and 99% confidence level. The t-statistics are stated in parentheses.

Multivariate Regressions for Daily S&P500 Straddle Excess Returns						
Maturity	1	2	3	6	9	12
Intercept	-0.0053 (-0.4764)	0.0008 (0.1288)	0.0016 (0.3540)	0.0013 (0.4370)	0.0012 (0.4828)	0.0005 (0.2435)
VVIX^{30D}	-0.0003 (-0.1883)	-0.0007 (-0.7390)	-0.0007 (-0.9210)	-0.0004 (-0.8884)	-0.0003 (-0.8782)	-0.0002 (-0.4871)
$\text{Slope}^{\text{VVIX}}$	0.0069^{***} (3.9135)	0.0029^{***} (3.0148)	0.0021^{***} (2.9604)	0.0014^{***} (2.9754)	0.0010^{***} (2.7216)	0.0008^{**} (2.4518)
$\text{Slope}^{\text{VIX}}$	-0.0034^{**} (-2.0377)	-0.0020^{**} (-2.2210)	-0.0016^{**} (-2.2493)	-0.0009^{**} (-2.0705)	-0.0008^{**} (-2.0904)	-0.0007^{**} (-2.0290)
VIX^{30D}	0.0019 (1.0078)	0.0012 (1.1780)	0.0011 (1.4040)	0.0008 (1.6368)	0.0006 (1.5673)	0.0004 (1.1765)
VRP	-0.0027 (-1.5087)	-0.0020^{**} (-1.9698)	-0.0016^{**} (-2.1458)	-0.0013^{***} (-2.6356)	-0.0008^{**} (-2.1558)	-0.0006^{*} (-1.8576)
$\text{r}_t^{\text{Straddle}}$	-0.0083^{***} (-5.1729)	-0.0014 (-1.5705)	0.0000 (0.0593)	0.0014^{***} (3.3413)	0.0019^{***} (5.4792)	0.0019^{***} (6.4074)
adj. R^2	0.0268	0.0135	0.0144	0.0258	0.0357	0.0394

Table 6: Regression: $\text{r}_{t+1}^{\text{Straddle}} = \alpha + \beta_1' X_t + \beta_2 \text{r}_t^{\text{Straddle}} + \epsilon_{t+1}$, where $\text{r}_{t+1}^{\text{Straddle}}$ is the daily excess return of a straddle on the S&P500 with maturities of $1, 2, 3, 6, 9$ and 12 months from end of day t to end of day $t+1$. X_t is a standardized vector of explanatory variables observed at the end of day t and which are defined as in Table 5. *,** and *** indicate statistical significance at the 90, 95, and 99% confidence level. The t-statistics are stated in parentheses.

Restricted Regressions for Daily VIX Straddle Excess Returns with Maturity of Two Months								
Panel A	(1)	(2)	(3)	(4)	(5)	(6)	(7)	(8)
Intercept	−0.0041	−0.0014*	−0.0014	−0.0022	0.0005	0.0059	−0.0014*	0.0058
	(−0.6764)	(−1.6500)	(−1.5966)	(−1.0618)	(0.4302)	(0.9059)	(−1.6509)	(0.8929)
$VVIX^{30D}$	0.0004					−0.0011		−0.0009
	(0.4485)					(−1.1392)		(−0.9043)
$Slope^{VVIX}$		0.0037***				0.0041***	0.0037***	0.0042***
		(3.9624)				(4.0985)	(3.9386)	(4.1037)
$Slope^{VIX}$			−0.0005				0.0003	0.0003
			(−0.5428)				(0.3418)	(0.2718)
VIX^{30D}				0.0004				−0.0005
				(0.4383)				(−0.5039)
VRP					−0.0024***			
					(−2.6261)			
$r_t^{Straddle}$	−0.0029***	−0.0040***	−0.0029***	−0.0029***	−0.0024***	−0.0039***	−0.0040***	−0.0039***
	(−3.2279)	(−4.3694)	(−3.2538)	(−3.2495)	(−2.6453)	(−4.1832)	(−4.3669)	(−4.1944)
adj. R^2	0.0049	0.0137	0.0050	0.0049	0.0087	0.0139	0.0132	0.0129
Restricted Regressions for Daily S&P500 Straddle Excess Returns with Maturity of Two Months								
Panel B	(1)	(2)	(3)	(4)	(5)	(6)	(7)	(8)
Intercept	−0.0052	−0.0017***	−0.0017***	−0.0040***	−0.0004	0.0014	−0.0017***	0.0018
	(−1.2331)	(−2.7405)	(−2.7162)	(−2.6393)	(−0.5265)	(0.2992)	(−2.7678)	(0.3975)
$VVIX^{30D}$	0.0005					−0.0005		−0.0007
	(0.8496)					(−0.6772)		(−0.8934)
$Slope^{VVIX}$		0.0024***				0.0026***	0.0020***	0.0021***
		(3.7421)				(3.7055)	(2.9945)	(2.9505)
$Slope^{VIX}$			−0.0025***				−0.0021***	−0.0021***
			(−4.0306)				(−3.3468)	(−3.2969)
VIX^{30D}				0.0011*				0.0003
				(1.6824)				(0.4919)
VRP					−0.0015**			
					(−2.4139)			
$r_t^{Straddle}$	0.0005	0.0000	0.0002	0.0004	0.0009	0.0000	−0.0003	−0.0002
	(0.7520)	(−0.0622)	(0.3315)	(0.6812)	(1.3500)	(0.0152)	(−0.3866)	(−0.3130)
adj. R^2	-0.0002	0.0073	0.0086	0.0001	0.0027	0.0070	0.0130	0.0124

Table 7: Rolling regression: $r_{t+1}^{Straddle} = \alpha + \beta_1 X_t + \beta_2 r_t^{Straddle} + \epsilon_t$, where $r_{t+1}^{Straddle}$ is the daily return of a straddle on the VIX (S&P500) with a maturity of two (one) months in panel A (B). X_t is a standardized vector of explanatory variables, which are calculated as for Table 5.

Parameter Estimates								
	σ_S	κ_V	σ_V	μ_V	λ_1	κ_q	σ_q	ρ_{Vq}
Estimate	0.3849	0.2988	0.8944	2.7428	0.1868	1.7828	9.9141	0.9477
Std. Err.	0.0005	0.0046	0.0038	0.1608	0.0105	0.0161	0.1415	0.0020

rel.RMSE: VVIX Term Structure				
$\text{VVIX}^{30\text{D}}$	$\text{VVIX}^{60\text{D}}$	$\text{VVIX}^{90\text{D}}$	$\text{VVIX}^{120\text{D}}$	$\text{VVIX}^{150\text{D}}$
5.1597	2.6271	2.7383	2.8950	3.5418

rel.RMSE: VIX Futures				
$\text{F}^{30\text{D}}$	$\text{F}^{60\text{D}}$	$\text{F}^{90\text{D}}$	$\text{F}^{120\text{D}}$	$\text{F}^{150\text{D}}$
6.5362	2.5791	2.0094	3.0781	4.6155

Table 8: The upper panel of the table shows the estimates of the structural model parameter estimates and their standard errors. Standard errors are estimated by the Outer-Product of the Gradient approach. The lower panels report the relative root mean squared pricing errors (rel.RMSE) of the model's VVIX term structure and of the VIX futures prices.

Relative Pricing Errors of the VVIX approximation					
	1 Month	2 Month	3 Month	4 Month	5 Month
mean($\epsilon^{\tau}_{\text{VVIX}}$)	0.0077	-0.0059	0.0122	0.0188	0.0212
std($\epsilon^{\tau}_{\text{VVIX}}$)	0.0123	0.0092	0.0141	0.0189	0.0229

Table 9: The table reports the accuracy for the closed form approximation of the VVIX term structure. To calculate the mean and standard deviation of the relative errors $\epsilon^{\tau}_{\text{VVIX}}$ we run 180,000 simulations for each Wednesday from 09/01/2007 to 08/31/2014.

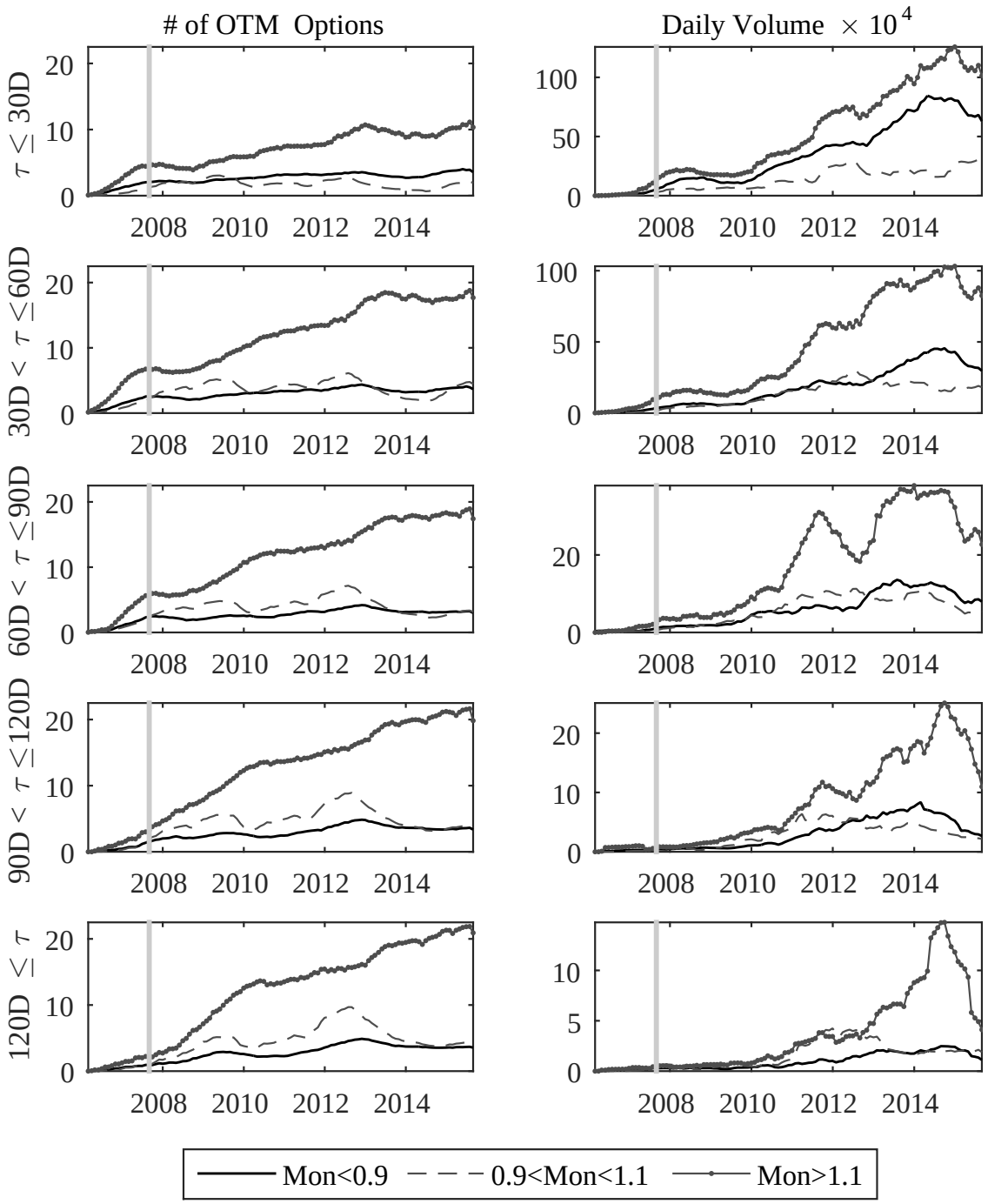

Figure 1: The figure displays the moving monthly averages of available OTM VIX options (left panels) and their trading volume (right panels) for different maturities and moneyness ranges. Moneyness is defined as the strike price divided by the VIX futures price. The grey vertical line marks the beginning of our data set period.

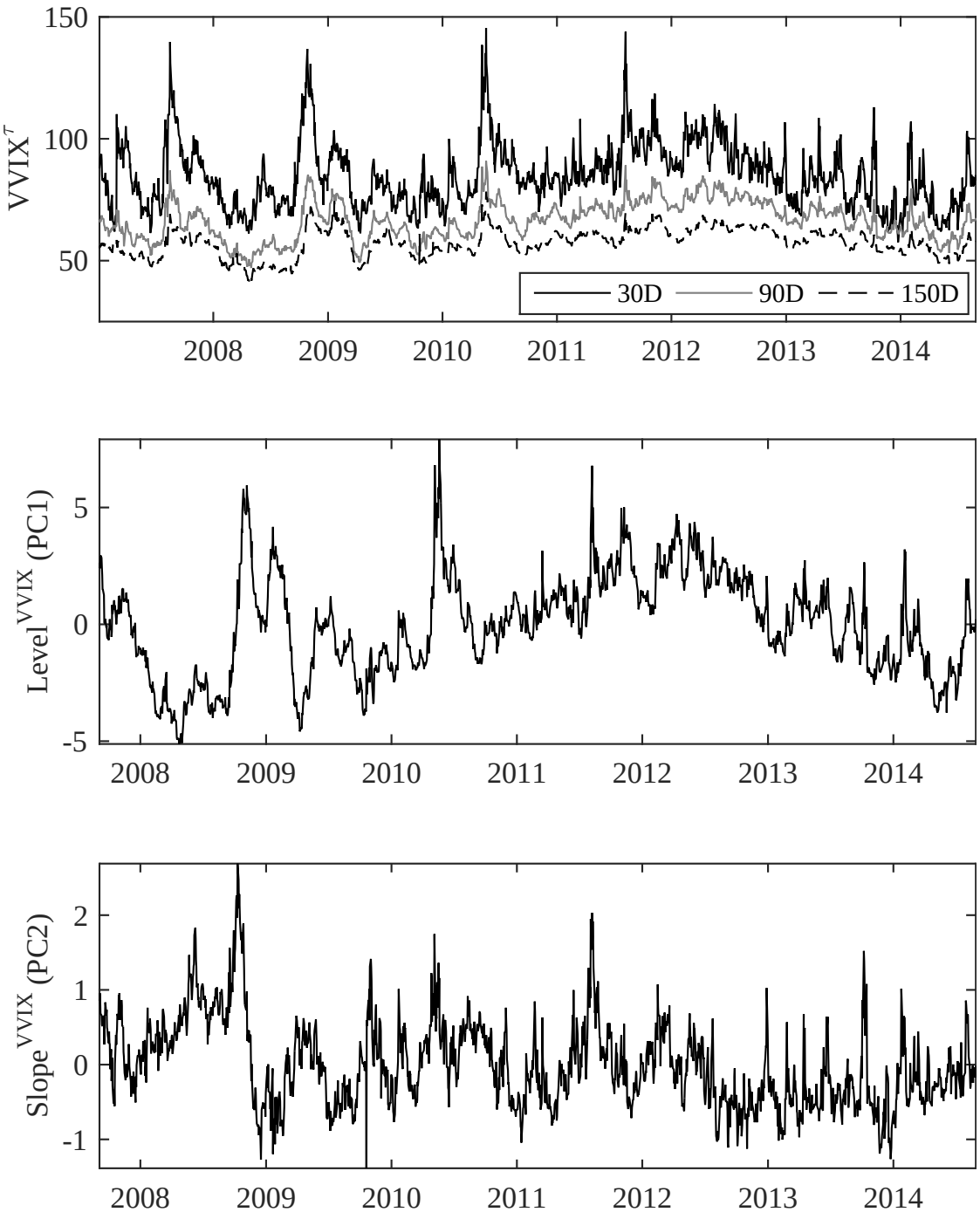

Figure 2: The figure depicts the VVIX for a maturity of 30, 90 and 150 days in the upper panel. The first and second principal component of the VVIX term structure, which we attribute to its level and slope, are shown in the middle and lower panel, respectively. Both components are normalized to a zero mean.

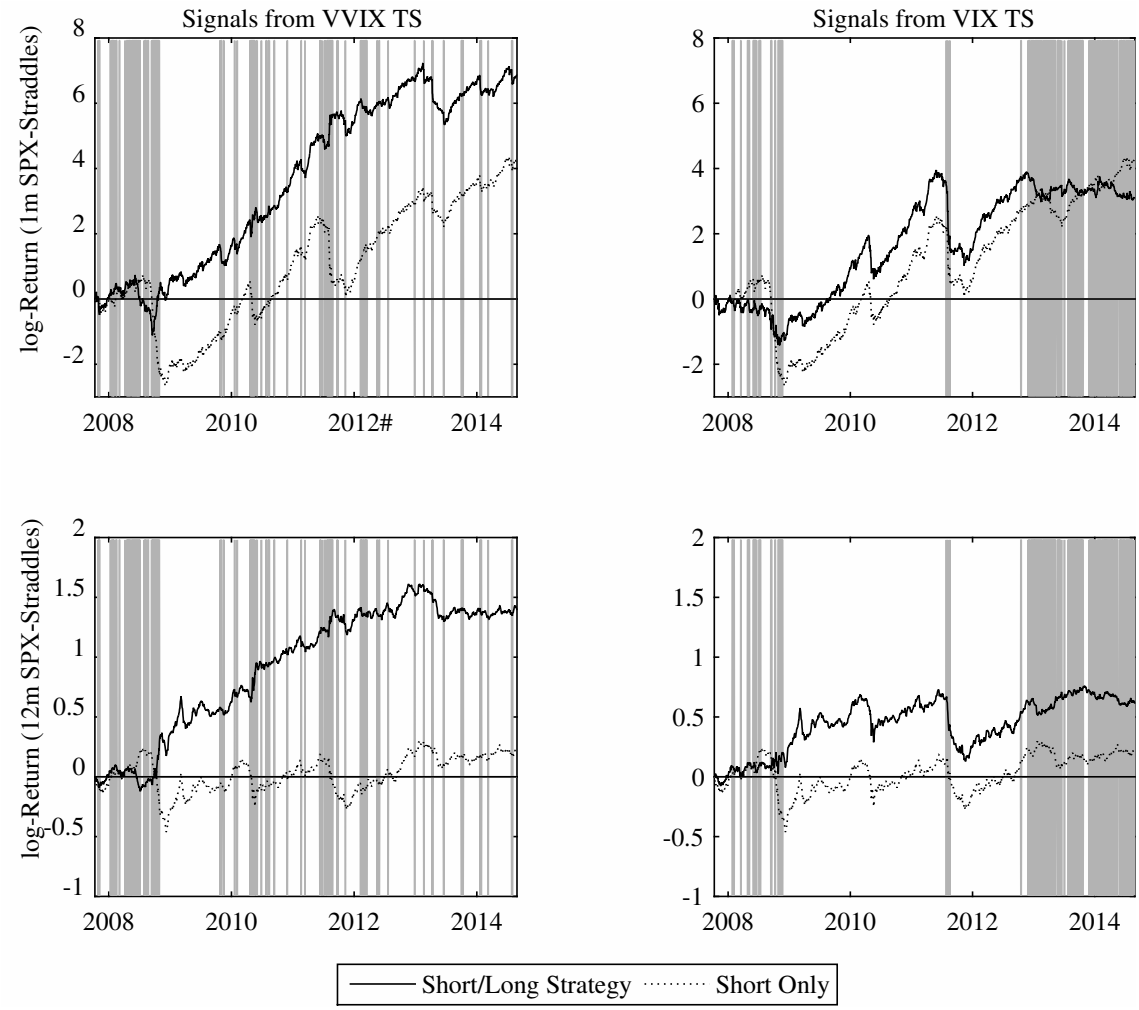

Figure 3: The figure shows logarithms of return paths for different S&P500 constant maturity straddle strategies. The left (right) panels show strategies which use a signal from the VVIX (VIX) term structure. In the top panels we plot strategies for one month straddles and in the bottom panel we plot strategies for twelve month straddles. The baseline strategy is going short in the straddles. If $\text{Slope}_t^{\text{VVIX}}$ ($\text{Slope}_t^{\text{VIX}}$) is in the highest (lowest) historic 75% quantile on day t, the strategy goes long straddles, which is marked by grey areas. The portfolios are adjusted on a daily basis and the second PCA components, and quantiles are calculated using only information until day t. The burn-in phase is one month (September '07) and trading costs are omitted.

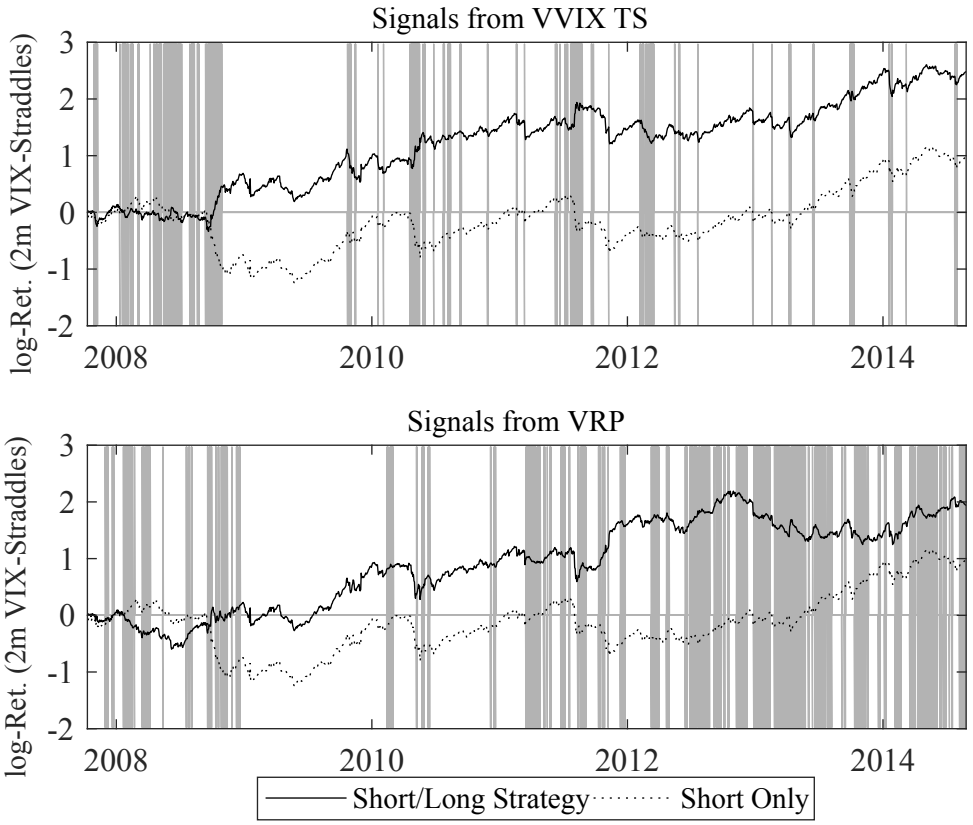

Figure 4: The figure shows logarithms of return paths for different two month constant maturity VIX straddle strategies. The panels show strategies which use a signal from $\text{Slope}^{\text{VVIX}}$ and the VRP. The baseline strategy is going short in the straddles. If the $\text{Slope}^{\text{VVIX}}$ (VRP) is in the highest (lowest) historic 75% quantile on day t, the strategy goes long straddles, which is marked by grey areas. The portfolios are adjusted on a daily basis and the quantile is calculated using only information until day t. The burn-in phase is one month (September '07) and trading costs are omitted.

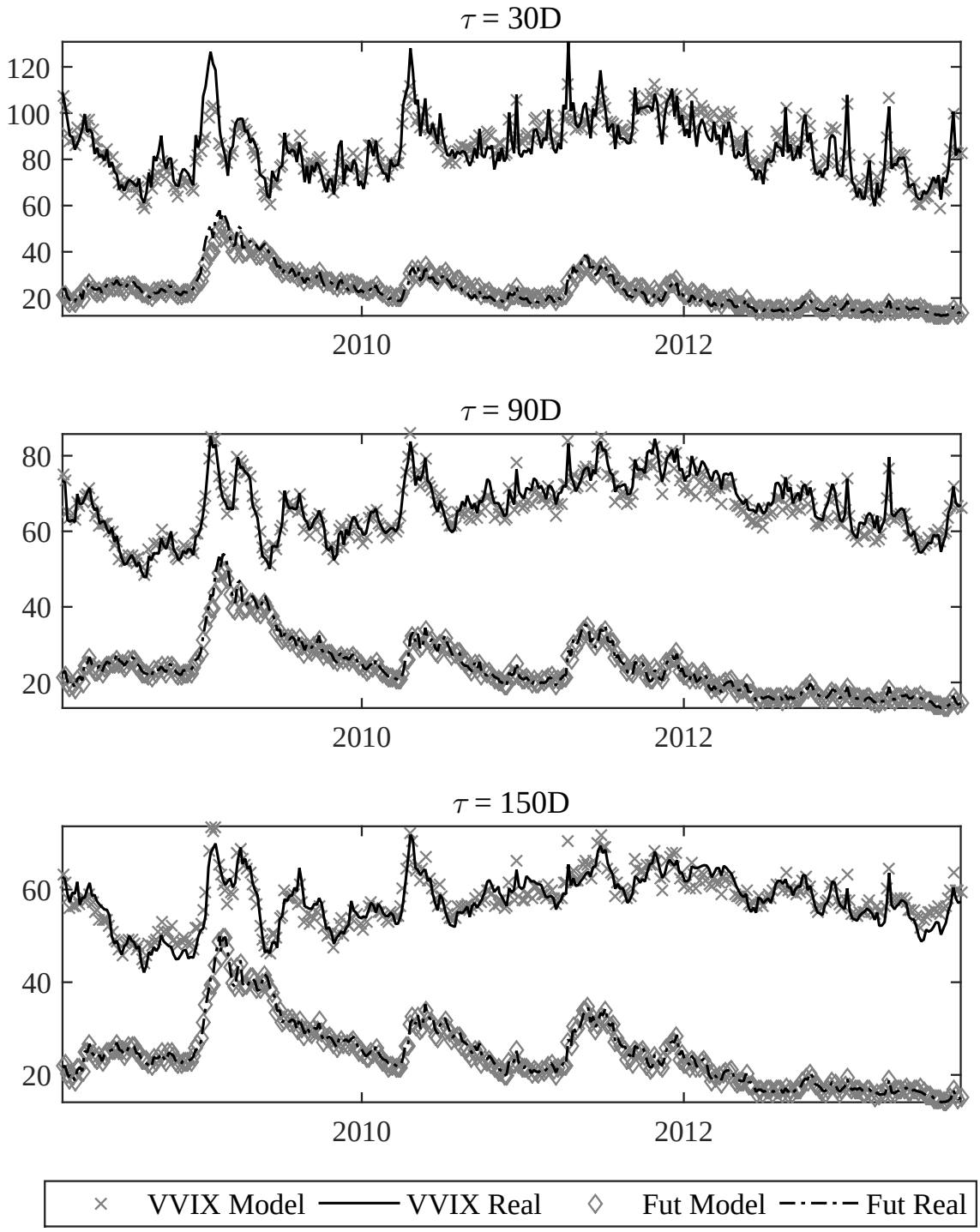

Figure 5: The figure shows the empirical and model-implied values of the VVIX term structure (top solid lines) and of the VIX futures prices (lower dashed lines). The plots for 60 and 120 days of maturity are omitted to save space.

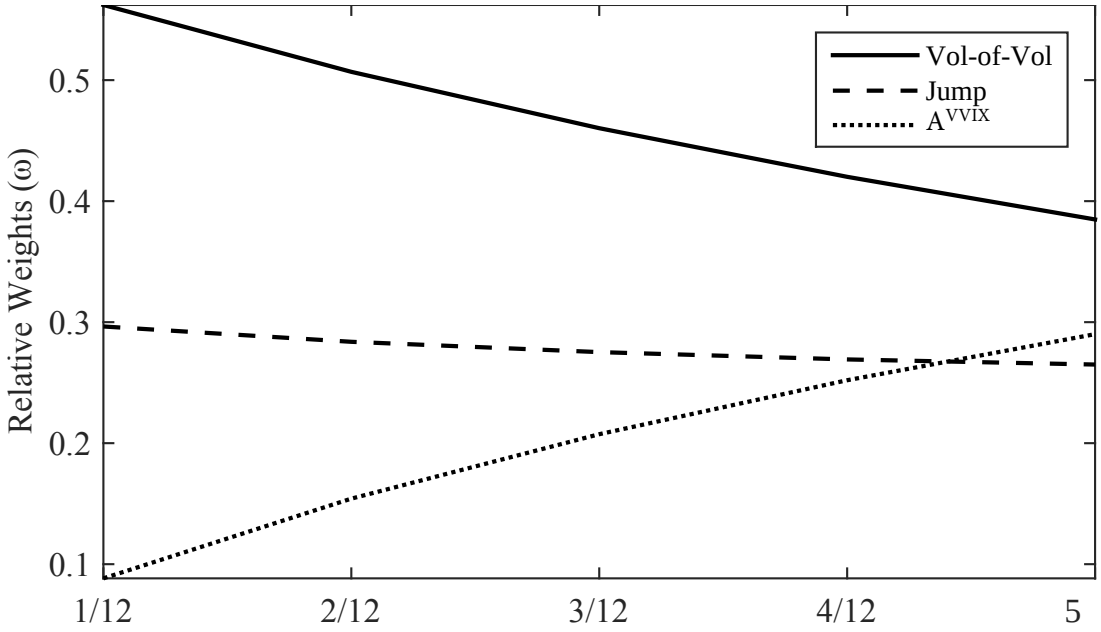

Figure 6: The figure shows the average of relative weights $\omega_t^\tau(X)$ of VVIX$^\tau$'s most important risk factors for different maturities measured in years.

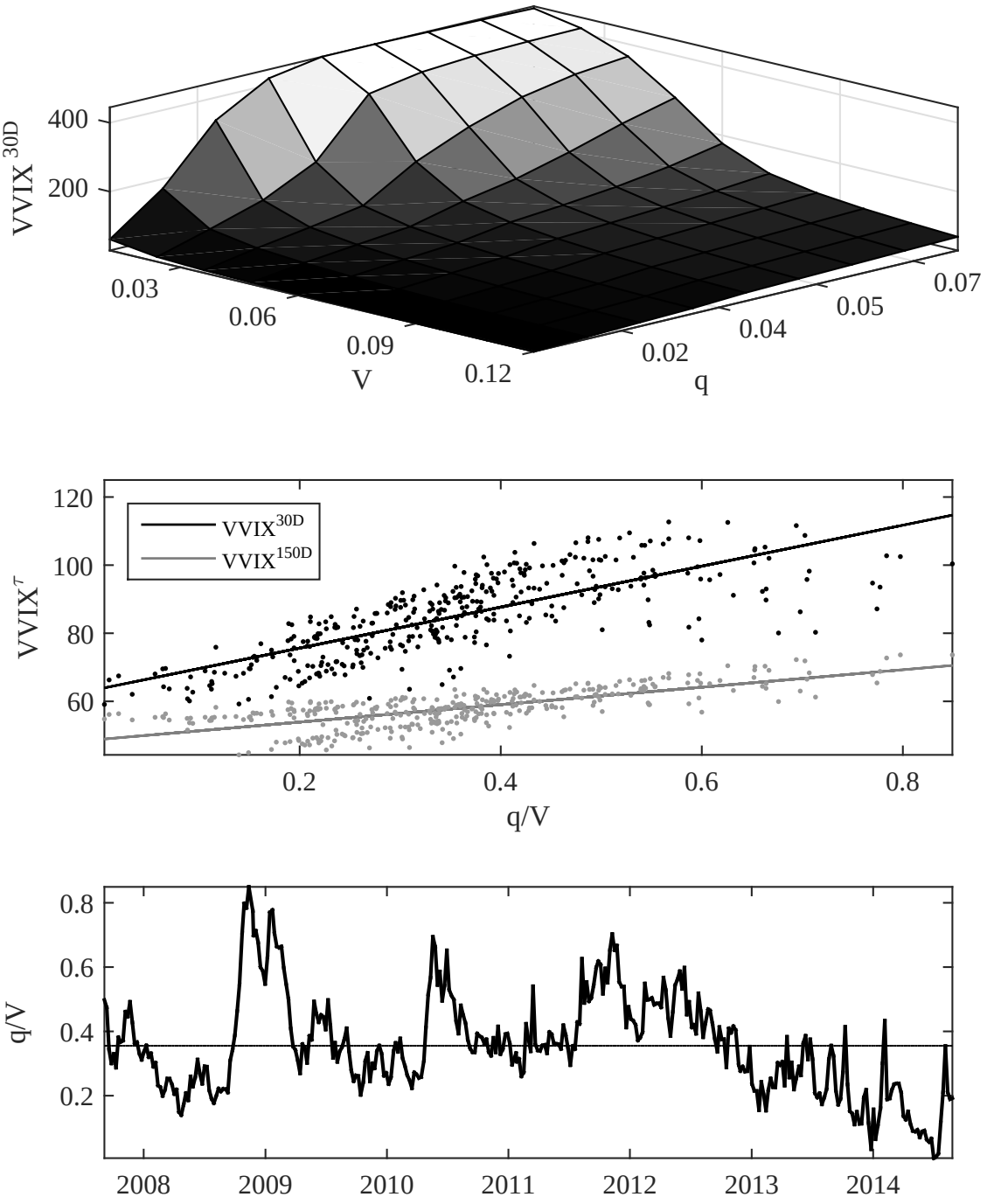

Figure 7: In the top panel we display the model-implied $\text{VVIX}^{30\text{D}}$ for different states of the economy V and q. The middle panel shows the empirical VVIX with maturity in 30D and 150D against the q/V-ratio, the bottom panel gives the estimated q/V-ratio. The q/V-ratio is rescaled by $\sigma_S^2\sigma_V^2$.

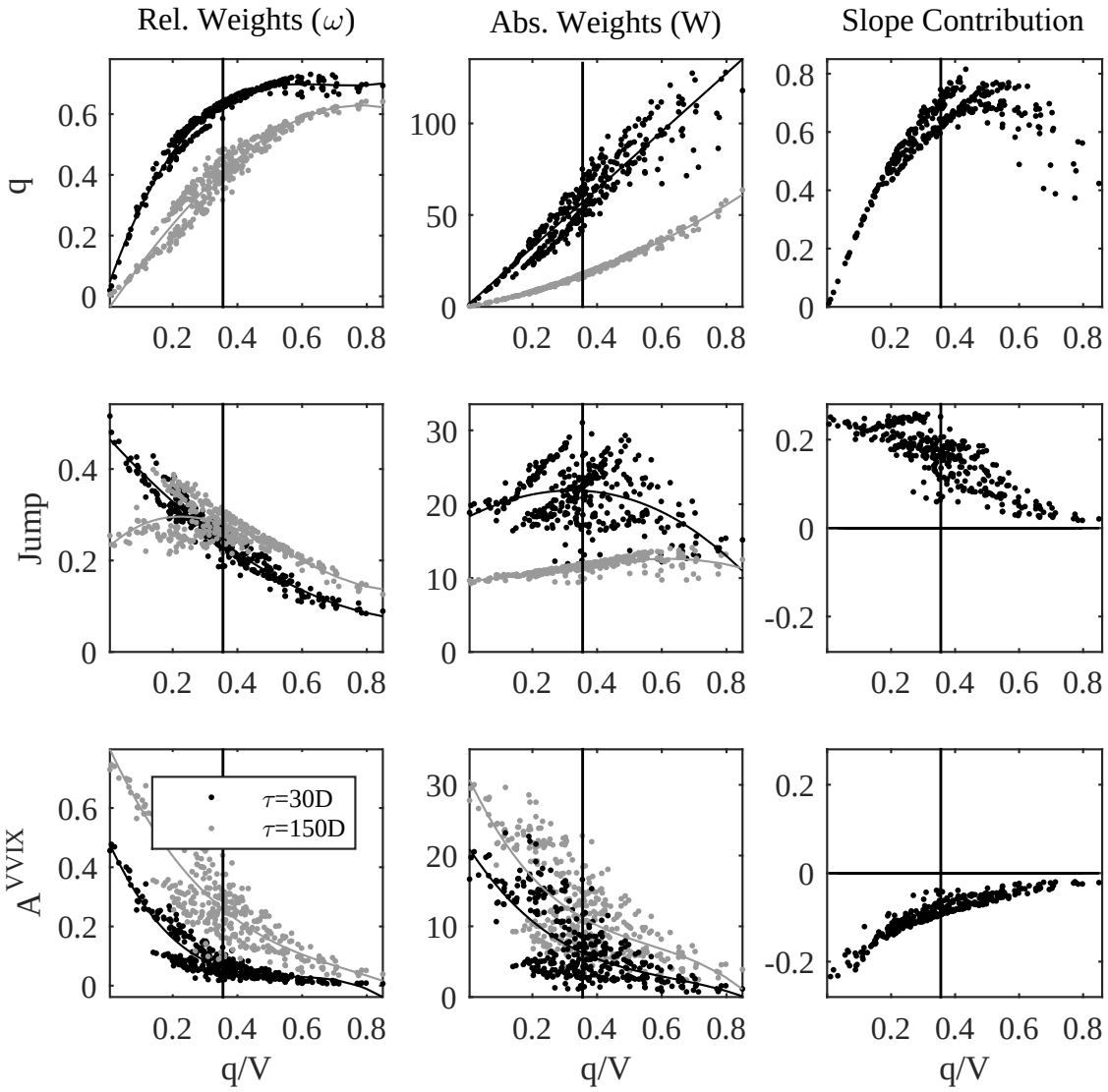

Figure 8: The figure shows the different risk-factor contributions to the $(\text{VVIX}_t^\tau)^2$ term structure as a function of the q/V-ratio. The first row shows the vol-of-vol risk contribution, the second row shows the jump-risk contribution and the last row shows A^{VVIX}. The relative contribution (ω_t^τ) is shown in the left panels, absolute contributions $(\text{W}_t^\tau \times 100)$ are plotted in the middle panels. The right panels give each factor's contribution to the slope, defined by $(W_t^{30\text{D}}(X) - W_t^{150\text{D}}(X))/\overline{\text{VVIX}_t^M}$. The vertical lines indicate the mean of our estimated q/V-ratio.

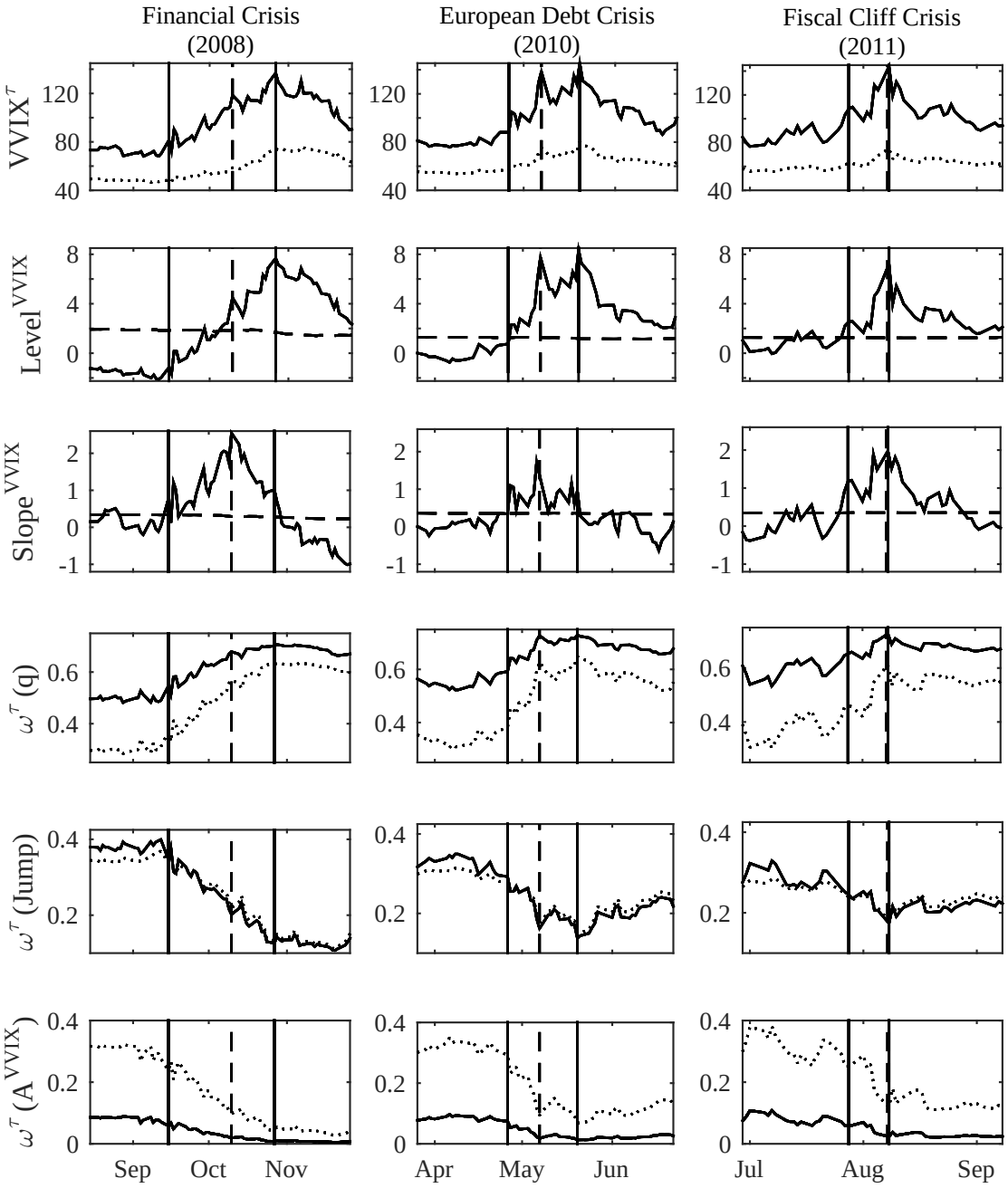

Figure 9: The figure depicts the VVIX for the longest and shortest maturity, $\text{Level}^{\text{VVIX}}$, $\text{Slope}^{\text{VVIX}}$ and the relative contribution of the vol-of-vol risk (q), jump risk and A^{VVIX} around crisis dates. In each plot the first vertical (solid) line marks the date where $\text{Slope}^{\text{VVIX}}$ is the first time in its 75% quantile and does not leave it until the crises' peak. The second vertical (dashed) lines mark the date when $\text{Slope}^{\text{VVIX}}$ was steepest. The third vertical (solid) lines mark the day where the $\text{VVIX}^{30\text{D}}$ peaked. The horizontal dashed lines in the $\text{Slope}^{\text{VVIX}}$ plots depict the triggering bound for the trading signal of Figure 3.

O Online Appendix

O.1 Additional Tables

Multivariat Regressions for Weekly S&P500 Straddle Excess Returns						
Maturity	1 Month	2 Months	3 Months	6 Months	9 Months	12 Months
Return Period	$\text{beta}^{\text{Slope}^{\text{VVIX}}}$					
1 Week	0.0045	0.0025	0.0019	0.0014	0.0010	0.0008
	(2.2855)	(2.2607)	(2.2677)	(2.1876)	(1.9360)	(1.7275)
2 Weeks	0.0043	0.0022	0.0018	0.0014	0.0011	0.0009
	(2.0612)	(1.9083)	(2.0920)	(2.0725)	(1.9092)	(1.7336)
3 Weeks	0.0040	0.0021	0.0017	0.0014	0.0011	0.0009
	(1.9320)	(1.8351)	(1.9427)	(2.1169)	(1.9156)	(1.7711)
	adj. R^2					
1 Week	0.0069	0.0096	0.0106	0.0141	0.0130	0.0112
2 Weeks	0.0078	0.0085	0.0108	0.0151	0.0148	0.0125
3 Weeks	0.0097	0.0101	0.0112	0.0155	0.0151	0.0126

Table O.1: Regression: $\text{r}_{t+1}^{\text{Straddle}} = \alpha + \beta' X_t + \epsilon_{t+1}$, where $\text{r}_{t+1}^{\text{Straddle}}$ is the excess return over one to three weeks of a delta-neutral S&P500 straddle with SPX option maturities of $1, 2, 3, 6, 9$ and 12 months. X_t is a standardized vector of explanatory variables observed at the end of day t and which are defined as in Table 5. Newey-West robust t-statistics are stated in parentheses.

Multivariat Regressions for Daily VIX Straddle Excess Returns					
Maturity	1 Month	2 Months	3 Months	4 Months	5 Months
Return Period	$\text{beta}^{\text{Slope}^{\text{VVIX}}}$				
2 Days	0.0103	0.0099	0.0102	0.0090	0.0083
	(0.2174)	(2.5502)	(2.8334)	(2.7316)	(1.6341)
3 Days	0.0148	0.0129	0.0136	0.0111	0.0100
	(0.3657)	(2.1520)	(2.7565)	(2.1222)	(1.3731)
4 Days	0.0230	0.0164	0.0175	0.0146	0.0104
	(0.7888)	(2.8275)	(2.7229)	(2.0803)	(0.9653)
5 Days	0.0012	0.0031	0.0036	0.0032	0.0021
	(0.4984)	(1.9608)	(2.1857)	(2.6891)	(2.0501)
	adj. R^2				
2 Days	0.0012	0.0208	0.0320	0.0638	0.0674
3 Days	0.0034	0.0266	0.0426	0.0529	0.0534
4 Days	0.0044	0.0299	0.0511	0.0715	0.0745
5 Days	0.0050	0.0371	0.0696	0.0902	0.0892

Table O.2: Regression: $\text{r}_{t+1}^{\text{Straddle}} = \alpha + \beta' X_t + \epsilon_{t+1}$, where $\text{r}_{t+1}^{\text{Straddle}}$ is the excess return over one to five days of a delta-neutral VIX straddle with VIX option maturities of 1 till 5 months. X_t is a standardized vector of explanatory variables observed at the end of day t and which are defined as in Table 5. Newey-West robust t-statistics are stated in parentheses.

Multivariat Regressions for Daily S&P500 Straddle Excess Returns						
Maturity	1 Month	2 Months	3 Months	6 Months	9 Months	12 Months
Lag	$\text{beta}^{\text{Slope}^{\text{VVIX}}}$					
2 Days	0.0052	0.0026	0.0019	0.0013	0.0010	0.0008
	(2.9172)	(2.7378)	(2.6076)	(2.7874)	(2.5714)	(2.4307)
3 Days	0.0045	0.0025	0.0019	0.0014	0.0010	0.0008
	(2.5468)	(2.6099)	(2.5737)	(2.8738)	(2.6851)	(2.4508)
	adj. R^2					
2 Days	0.0126	0.0125	0.0149	0.0230	0.0273	0.0263
3 Days	0.0071	0.0096	0.0110	0.0141	0.0136	0.0114

Table O.3: Regression: $\text{r}_{t+lag}^{\text{Straddle}} = \alpha + \beta' X_t + \beta_2 \text{r}_t^{\text{Straddle}} + \epsilon_{t+1}$, where $\text{r}_{t+1}^{\text{Straddle}}$ is the daily excess return of a straddle on the S&P500 with maturities of $1, 2, 3, 6, 9$ and 12 months from end of day $t + lagged\ days$ to end of day $t + lagged\ days + 1$. X_t is a standardized vector of explanatory variables observed at the end of day t and which are defined as in Table 5. The t-statistics are stated in parentheses.

Multivariat Regressions for Daily VIX Straddle Excess Returns					
Maturity	1 Month	2 Months	3 Months	4 Months	5 Months
Lag	$\text{beta}^{\text{Slope}^{\text{VVIX}}}$				
2 Days	0.0012	0.0031	0.0033	0.0023	0.0083
	(0.5164)	(2.9519)	(3.8773)	(2.7316)	(1.6341)
3 Days	0.0008	0.0015	0.0032	0.0027	0.0013
	(0.3437)	(2.9124)	(3.7593)	(3.4209)	(1.3731)
	adj. R^2				
2 Days	-0.0019	0.0056	0.0132	0.0344	0.0287
3 Days	-0.0021	0.0042	0.0113	0.0433	0.0373

Table O.4: Regression: $\text{r}_{t+lag}^{\text{Straddle}} = \alpha + \beta_1' X_t + \beta_2 \text{r}_t^{\text{Straddle}} + \epsilon_{t+1}$, where $\text{r}_{t+1}^{\text{Straddle}}$ is the daily excess return of a straddle on the VIX with maturities of $1, 2, 3, 4$ and 5 months from end of day $t+lagged\ days$ to end of day $t+lagged\ days+1$. X_t is a standardized vector of explanatory variables observed at the end of day t and which are defined as in Table 5. t-statistics are stated in parentheses.

Restricted Regressions for Daily S&P500 Straddle Excess Returns with Maturity of One Month								
	(1)	(2)	(3)	(4)	(5)	(6)	(7)	(8)
Intercept	-0.0264^{**}	-0.0056^{***}	-0.0056^{***}	-0.0127^{***}	-0.0036^{*}	-0.0062	-0.0056^{***}	-0.0052
	(-2.5565)	(-3.6805)	(-3.6732)	(-3.4532)	(-1.8299)	(-0.558)	(-3.7141)	(-0.4668)
VVIX	0.0032^{**}					0.0001		-0.0003
	(2.0447)					(0.0615)		(-0.1572)
$\text{Slope}^{\text{VVIX}}$		0.0078^{***}				0.0077^{***}	0.0069^{***}	0.0068^{***}
		(4.9477)				(4.499)	(4.3237)	(3.8796)
$\text{Slope}^{\text{VIX}}$			-0.0057^{***}				-0.0044^{***}	-0.0043^{***}
			(-3.7176)				(-2.8421)	(-2.7802)
VIX				0.0033^{**}				0.0007
				(2.1474)				(0.3917)
VRP					-0.0024			
					(-1.5053)			
$\text{r}_t^{\text{Straddle}}$	-0.0070^{***}	-0.0083^{***}	-0.0071^{***}	-0.0068^{***}	-0.0060^{***}	-0.0083^{***}	-0.0087^{***}	-0.0087^{***}
	(-4.5205)	(-5.3345)	(-4.6533)	(-4.4605)	(-3.8584)	(-5.3115)	(-5.5519)	(-5.5262)
adj. R^2	0.01150	0.0231	0.0170	0.0117	0.0104	0.0225	0.0271	0.0261

Table O.5: Rolling regression: $\text{r}_{t+1}^{\text{Straddle}} = \alpha + \beta_1' X_t + \beta_2 \text{r}_t^{\text{Straddle}} + \epsilon_{t+1}$, where $\text{r}_{t+1}^{\text{Straddle}}$ is the daily excess return of a straddle on the S&P500 with a maturity of one month from end of day t to end of day $t+1$. X_t is a vector of explanatory variables observed at the end of day t. VVIX^{30D} is the implied volatility-of-volatility index, $\text{Slope}^{\text{VVIX}}$ is the second PCA component of the VVIX term structure, $\text{Slope}^{\text{VIX}}$ is the second PCA component of the VIX term structure, VIX^{30D} is the volatility index and the variance risk premia (VRP) is calculated as the differential of the risk-neutral and the physical expectation of the variation of the stock index over the next 30 days. We define $\text{VRP}_t \equiv \mathbb{E}_t^{\mathbb{Q}} \int_0^{\text{30D}} (d \ln S_{t+u})^2 du - \mathbb{E}_t^{\mathbb{P}} \int_0^{\text{30D}} (d \ln S_{t+u})^2 du = \text{VIX}_t^{\text{30D}} - \text{RV}_t$, where $\text{RV}_t = \sum_{j=1}^{21} \sum_i (r_{t-j,i})^2$ and $r_{t-j,i}$ are the ith five-minute log-returns at day $t-j$. For the regressions we use daily data samples from 09/01/2007 to 08/31/2014. *,** and *** indicate statistical significance at the 90, 95, and 99% confidence level. The t-statistics are stated in parentheses.

Multivariat Regressions for Daily S&P500 Straddle Excess Returns with Maturity of Three Months								
	(1)	(2)	(3)	(4)	(5)	(6)	(7)	(8)
Intercept	-0.0052	-0.0017^{***}	-0.0017^{***}	-0.0040^{***}	-0.0004	0.0014	-0.0017^{***}	0.0018
	(-1.2331)	(-2.7405)	(-2.7162)	(-2.6393)	(-0.5265)	(0.2992)	(-2.7678)	(0.3975)
VVIX^{30D}	0.0005					-0.0005		-0.0007
	(0.8496)					(-0.6772)		(-0.8934)
$\text{Slope}^{\text{VVIX}}$		0.0024^{***}				0.0026^{***}	0.002^{***}	0.0021^{***}
		(3.7421)				(3.7055)	(2.9945)	(2.9505)
$\text{Slope}^{\text{VIX}}$			-0.0025^{***}				-0.0021^{***}	-0.0021^{***}
			(-4.0306)				(-3.3468)	(-3.2969)
VIX^{30D}				0.0011^{*}				0.0003
				(1.6824)				(0.4919)
VRP					-0.0015^{**}			
					(-2.4139)			
$\text{r}_t^{\text{Straddle}}$	0.0005	0.0000	0.0002	0.0004	0.0009	0.0000	-0.0003	-0.0002
	(0.7520)	(-0.0622)	(0.3315)	(0.6812)	(1.35)	(0.0152)	(-0.3866)	(-0.3130)
adj. R^2	-0.0002	0.0073	0.0086	0.0010	0.0027	0.0070	0.0130	0.0124

Table O.6: Rolling regression: $\text{r}_{t+1}^{\text{Straddle}} = \alpha + \beta_1' X_t + \beta_2 \text{r}_t^{\text{Straddle}} + \epsilon_{t+1}$, where $\text{r}_{t+1}^{\text{Straddle}}$ is the daily excess return of a straddle on the S&P500 with a maturity of three months from end of day t to end of day $t+1$. X_t is a vector of explanatory variables observed at the end of day t. VVIX^{30D} is the implied volatility-of-volatility index, $\text{Slope}^{\text{VVIX}}$ is the second PCA component of the VVIX term structure, $\text{Slope}^{\text{VIX}}$ is the second PCA component of the VIX term structure, VIX^{30D} is the volatility index and the variance risk premium (VRP) is calculated as the differential of the risk-neutral and the physical expectation of the variation of the stock index over the next 30 days. We define $\text{VRP}_t \equiv \mathbb{E}_t^{\mathbb{Q}} \int_0^{\text{30D}} (d \ln S_{t+u})^2 du - \mathbb{E}_t^{\mathbb{P}} \int_0^{\text{30D}} (d \ln S_{t+u})^2 du = \text{VIX}_t^{\text{30D}} - \text{RV}_t$, where $\text{RV}_t = \sum_{j=1}^{21} \sum_i (r_{t-j,i})^2$ and $r_{t-j,i}$ are the ith five-minute log-returns at day $t-j$. For the regressions we use daily data samples from 09/01/2007 to 08/31/2014. *,** and *** indicate statistical significance at the 90, 95, and 99% confidence level. The t-statistics are stated in parentheses.

Multivariat Regressions for Excess Daily S&P500 Straddle Returns with Maturity of Six Months								
	(1)	(2)	(3)	(4)	(5)	(6)	(7)	(8)
Intercept	-0.0031	-0.0007^{*}	-0.0007^{*}	-0.0022^{**}	0.0002	0.0012	-0.0007^{*}	0.0015
	(-1.1335)	(-1.7076)	(-1.6907)	(-2.2519)	(0.4635)	(0.4005)	(-1.7239)	(0.5016)
$\text{VVIX}^{30\text{D}}$	0.0004					-0.0003		-0.0004
	(0.8987)					(-0.6378)		(-0.8632)
$\text{Slope}^{\text{VVIX}}$		0.0016^{***}				0.0017^{***}	0.0013^{***}	0.0014^{***}
		(3.7616)				(3.7065)	(3.0068)	(2.9444)
$\text{Slope}^{\text{VIX}}$			-0.0017^{***}				-0.0014^{***}	-0.0014^{***}
			(-4.0283)				(-3.3334)	(-3.2810)
$\text{VIX}^{30\text{D}}$				0.0007^{*}				0.0002
				(1.7165)				(0.5103)
VRP					-0.0011^{***}			
					(-2.7691)			
$\text{r}_t^{\text{Straddle}}$	0.0017^{***}	0.0014^{***}	0.0015^{***}	0.0017^{***}	0.0019^{***}	0.0014^{***}	0.0012^{***}	0.0013^{***}
	(4.0775)	(3.2691)	(3.7449)	(4.0420)	(4.7251)	(3.3199)	(2.9589)	(3.0021)
adj. R^2	0.0100	0.0175	0.0187	0.0112	0.0139	0.0172	0.0231	0.0225

Table O.7: Rolling regression: $\text{r}_{t+1}^{\text{Straddle}} = \alpha + \beta_1' X_t + \beta_2 \text{r}_t^{\text{Straddle}} + \epsilon_{t+1}$, where $\text{r}_{t+1}^{\text{Straddle}}$ is the daily excess return of a straddle on the S&P500 with a maturity of six months from end of day t to end of day $t+1$. X_t is a vector of explanatory variables observed at the end of day t. $\text{VVIX}^{30\text{D}}$ is the implied volatility-of-volatility index, $\text{Slope}^{\text{VVIX}}$ is the second PCA component of the VVIX term structure, $\text{Slope}^{\text{VIX}}$ is the second PCA component of the VIX term structure, $\text{VIX}^{30\text{D}}$ is the volatility index and the variance risk premium (VRP) is calculated as the differential of the risk-neutral and the physical expectation of the variation of the stock index over the next 30 days. We define $\text{VRP}_t \equiv \mathbb{E}_t^{\mathbb{Q}} \int_0^{30\text{D}} (d \ln S_{t+u})^2 du - \mathbb{E}_t^{\mathbb{P}} \int_0^{30\text{D}} (d \ln S_{t+u})^2 du = \text{VIX}_t^{30\text{D}} - \text{RV}_t$, where $\text{RV}_t = \sum_{j=1}^{21} \sum_i (r_{t-j,i})^2$ and $r_{t-j,i}$ are the ith five-minute log-returns at day $t-j$. For the regressions we use daily data samples from 09/01/2007 to 08/31/2014. *,** and *** indicate statistical significance at the 90, 95, and 99% confidence level. The t-statistics are stated in parentheses.

Multivariat Regressions for Daily S&P500 Straddle Excess Returns with Maturity of Nine Months								
	(1)	(2)	(3)	(4)	(5)	(6)	(7)	(8)
Intercept	-0.0022	-0.0003	-0.0003	-0.0016^{**}	0.0003	0.0011	-0.0003	0.0013
	(-0.9988)	(-1.0073)	(-0.9982)	(-2.0446)	(0.6290)	(0.4439)	(-1.0148)	(0.5479)
$\text{VVIX}^{30\text{D}}$	0.0003					-0.0002		-0.0003
	(0.8630)					(-0.5859)		(-0.8676)
$\text{Slope}^{\text{VVIX}}$		0.0012^{***}				0.0013^{***}	0.0009^{***}	0.0010^{***}
		(3.5054)				(3.4463)	(2.7690)	(2.6801)
$\text{Slope}^{\text{VIX}}$			-0.0013^{***}				-0.0011^{***}	-0.0010^{***}
			(-3.8257)				(-3.1635)	(-3.0943)
$\text{VIX}^{30\text{D}}$				0.0006^{*}				0.0002
				(1.7980)				(0.6745)
VRP					-0.0007^{**}			
					(-2.2135)			
$\text{r}_t^{\text{Straddle}}$	0.0021^{***}	0.0019^{***}	0.0020^{***}	0.0020^{***}	0.0022^{***}	0.0019^{***}	0.0018^{***}	0.0018^{***}
	(6.2319)	(5.5362)	(5.9919)	(6.1930)	(6.7399)	(5.5661)	(5.2771)	(5.2914)
adj. R^2	0.0230	0.0293	0.0306	0.0243	0.0253	0.0290	0.0343	0.0337

Table O.8: Rolling regression: $\text{r}_{t+1}^{\text{Straddle}} = \alpha + \beta_1' X_t + \beta_2 \text{r}_t^{\text{Straddle}} + \epsilon_{t+1}$, where $\text{r}_{t+1}^{\text{Straddle}}$ is the daily excess return of a straddle on the S&P500 with a maturity of one year from end of day t to end of day $t+1$. X_t is a vector of explanatory variables observed at the end of day t. $\text{VVIX}^{30\text{D}}$ is the implied volatility-of-volatility index, $\text{Slope}^{\text{VVIX}}$ is the second PCA component of the VVIX term structure, $\text{Slope}^{\text{VIX}}$ is the second PCA component of the VIX term structure, $\text{VIX}^{30\text{D}}$ is the volatility index and the variance risk premium (VRP) is calculated as the differential of the risk-neutral and the physical expectation of the variation of the stock index over the next 30 days. We define $\text{VRP}_t \equiv \mathbb{E}_t^{\mathbb{Q}} \int_0^{30\text{D}} (d \ln S_{t+u})^2 du - \mathbb{E}_t^{\mathbb{P}} \int_0^{30\text{D}} (d \ln S_{t+u})^2 du = \text{VIX}_t^{30\text{D}} - \text{RV}_t$, where $\text{RV}_t = \sum_{j=1}^{21} \sum_i (r_{t-j,i})^2$ and $r_{t-j,i}$ are the ith five-minute log-returns at day $t-j$. For the regressions we use daily data samples from 09/01/2007 to 08/31/2014. *,** and *** indicate statistical significance at the 90, 95, and 99% confidence level. The t-statistics are stated in parentheses.

Multivariat Regressions for Daily S&P500 Straddle Excess Returns with Maturity of One Year								
	(1)	(2)	(3)	(4)	(5)	(6)	(7)	(8)
Intercept	-0.0022	-0.0002	-0.0002	-0.0011	0.0003	0.0004	-0.0002	0.0007
	(-1.1199)	(-0.5315)	(-0.5267)	(-1.6327)	(0.8268)	(0.2073)	(-0.5336)	(0.3067)
VVIX^{30D}	0.0003					-0.0001		-0.0002
	(1.0543)					(-0.2820)		(-0.4836)
$\text{Slope}^{\text{VVIX}}$		0.0010^{***}				0.0010^{***}	0.0008^{**}	0.0008^{**}
		(3.2583)				(3.0941)	(2.5539)	(2.4065)
$\text{Slope}^{\text{VIX}}$			-0.0010^{***}				-0.0009^{***}	-0.0009^{***}
			(-3.5783)				(-2.9502)	(-2.9019)
VIX^{30D}				0.0005				0.0001
				(1.5569)				(0.3858)
VRP					-0.0006^{**}			
					(-1.9643)			
$\text{r}_t^{\text{Straddle}}$	0.0021^{***}	0.0019^{***}	0.0020^{***}	0.0021^{***}	0.0022^{***}	0.0019^{***}	0.0019^{***}	0.0019^{***}
	(7.0514)	(6.5110)	(6.9325)	(7.1183)	(7.5140)	(6.5030)	(6.3059)	(6.2992)
adj. R^2	0.0295	0.0348	0.0359	0.0303	0.0310	0.0342	0.0390	0.0380

Table O.9: Rolling regression: $\text{r}_{t+1}^{\text{Straddle}} = \alpha + \beta_1' X_t + \beta_2 \text{r}_t^{\text{Straddle}} + \epsilon_{t+1}$, where $\text{r}_{t+1}^{\text{Straddle}}$ is the daily excess return of a straddle on the S&P500 with a maturity of one year from end of day t to end of day $t+1$. X_t is a vector of explanatory variables observed at the end of day t. VVIX^{30D} is the implied volatility-of-volatility index, $\text{Slope}^{\text{VVIX}}$ is the second PCA component of the VVIX term structure, $\text{Slope}^{\text{VIX}}$ is the second PCA component of the VIX term structure, VIX^{30D} is the volatility index and the variance risk premium (VRP) is calculated as the differential of the risk-neutral and the physical expectation of the variation of the stock index over the next 30 days. We define $\text{VRP}_t \equiv \mathbb{E}_t^{\mathbb{Q}} \int_0^{30\text{D}} (d \ln S_{t+u})^2 du - \mathbb{E}_t^{\mathbb{P}} \int_0^{30\text{D}} (d \ln S_{t+u})^2 du = \text{VIX}_t^{30\text{D}} - \text{RV}_t$, where $\text{RV}_t = \sum_{j=1}^{21} \sum_i (r_{t-j,i})^2$ and $r_{t-j,i}$ are the ith five-minute log-returns at day $t-j$. For the regressions we use daily data samples from 09/01/2007 to 08/31/2014. *,** and *** indicate statistical significance at the 90, 95, and 99% confidence level. The t-statistics are stated in parentheses.

Restricted Regressions for Daily VIX Straddle Excess Returns with Maturity of One Month								
	(1)	(2)	(3)	(4)	(5)	(6)	(7)	(8)
Intercept	0.0080	-0.0037^{*}	-0.0037^{*}	0.0001	-0.0014	0.0093	-0.0037^{*}	0.0095
	(0.6003)	(-1.9115)	(-1.9270)	(0.0219)	(-0.5764)	(0.6469)	(-1.9221)	(0.6585)
$\text{VVIX}^{30\text{D}}$	-0.0018					-0.0020		-0.0014
	(-0.8889)					(-0.9121)		(-0.6250)
$\text{Slope}^{\text{VVIX}}$		-0.0003				0.0005	-0.0007	0.0004
		(-0.1268)				(0.2418)	(-0.3237)	(0.1911)
$\text{Slope}^{\text{VIX}}$			-0.0016				-0.0017	-0.0020
			(-0.8287)				(-0.8804)	(-1.0271)
$\text{VIX}^{30\text{D}}$				-0.0018				-0.0017
				(-0.9215)				(-0.7838)
VRP					-0.0028			
					(-1.4787)			
$\text{r}_t^{\text{Straddle}}$	-0.0026	-0.0030	-0.0031	-0.0029	-0.0026	-0.0027	-0.0030	-0.0028
	(-1.3191)	(-1.4633)	(-1.6016)	(-1.4795)	(-1.3218)	(-1.3406)	(-1.4715)	(-1.3924)
adj. R^2	0.0007	0.0003	0.0007	0.0008	0.0016	0.0002	0.0001	-0.0002

Table O.10: Rolling regression: $\text{r}_{t+1}^{\text{Straddle}} = \alpha + \beta_1 X_t + \beta_2 \text{r}_t^{\text{Straddle}} + \epsilon_t$, where $\text{r}_{t+1}^{\text{Straddle}}$ is the is the daily return of a straddle on the VIX with a maturity of one month from end of day t to end of day $t+1$. X_t is a vector of explanatory variables observed at the end of day t. VVIX is the implied volatility-of-volatility index, $\text{Slope}^{\text{VVIX}}$ is the second PCA component of the VVIX term structure, VIX is CBOE's volatility index, $\text{Slope}^{\text{VVX}}$ is the second PCA component of the VIX term structure and the variance risk premium (VRP) is calculated as the differential of the risk-neutral and the physical expectation of the variation of the stock index over the next 30 days. We define $\text{VRP}_t \equiv \mathbb{E}_t^{\mathbb{Q}} \int_0^{30\text{D}} (d \ln S_{t+u})^2 du - \mathbb{E}_t^{\mathbb{P}} \int_0^{30\text{D}} (d \ln S_{t+u})^2 du = \text{VIX}_t - \text{RV}_t$, where $\text{RV}_t = \sum_{j=1}^{21} \sum_i (r_{t-j,i})^2$ and $r_{t-j,i}$ are the ith five-minute log-returns at day $t-j$. For the regressions we use daily data samples from 09/01/2007 to 08/31/2014. *,** and *** indicate statistical significance at the 90, 95, and 99% confidence level. The t-statistics are stated in parentheses.

Restricted Regressions for Daily VIX Straddle Excess Returns with Maturity of Three Months								
	(1)	(2)	(3)	(4)	(5)	(6)	(7)	(8)
Intercept	-0.0068	-0.0003	-0.0004	-0.0032^{*}	0.0011	0.0045	-0.0003	0.0042
	(-1.4221)	(-0.4164)	(-0.5266)	(-1.865)	(1.2336)	(0.8536)	(-0.4192)	(0.8009)
VVIX^{30D}	0.0010					-0.0007		-0.0007
	(1.3595)					(-0.9169)		(-0.8251)
$\text{Slope}^{\text{VVIX}}$		0.0039^{***}				0.0042^{***}	0.0037^{***}	0.0040^{***}
		(5.272)				(5.1723)	(4.9862)	(4.7677)
$\text{Slope}^{\text{VIX}}$			-0.0014^{*}				-0.0007	-0.0006
			(-1.8965)				(-0.8517)	(-0.7826)
VIX^{30D}				0.0014^{*}				0.0000
				(1.8066)				(0.0428)
VRP					-0.0020^{**}			
					(-2.4651)			
$\text{r}_t^{\text{Straddle}}$	-0.0012^{*}	-0.0023^{***}	-0.0011	-0.0012^{*}	-0.0005	-0.0022^{***}	-0.0023^{***}	-0.0022^{***}
	(-1.6798)	(-3.1029)	(-1.5663)	(-1.649)	(-0.7178)	(-2.9338)	(-3.1369)	(-2.9695)
adj. R^2	0.0011	0.0175	0.0022	0.0020	0.0038	0.0174	0.0174	0.0166

Table O.11: Rolling regression: $\text{r}_{t+1}^{\text{Straddle}} = \alpha + \beta_1 X_t + \beta_2 \text{r}_t^{\text{Straddle}} + \epsilon_t$, where $\text{r}_{t+1}^{\text{Straddle}}$ is the is the daily return of a straddle on the VIX with a maturity of three months from end of day t to end of day $t+1$. X_t is a vector of explanatory variables observed at the end of day t. VVIX is the implied volatility-of-volatility index, $\text{Slope}^{\text{VVIX}}$ is the second PCA component of the VVIX term structure, VIX is CBOE's volatility index, $\text{Slope}^{\text{VVX}}$ is the second PCA component of the VIX term structure and the variance risk premium (VRP) is calculated as the differential of the risk-neutral and the physical expectation of the variation of the stock index over the next 30 days. We define $\text{VRP}_t \equiv \mathbb{E}_t^{\mathbb{Q}} \int_0^{30\text{D}} (d \ln S_{t+u})^2 du - \mathbb{E}_t^{\mathbb{P}} \int_0^{30\text{D}} (d \ln S_{t+u})^2 du = \text{VIX}_t - \text{RV}_t$, where $\text{RV}_t = \sum_{j=1}^{21} \sum_i (r_{t-j,i})^2$ and $r_{t-j,i}$ are the ith five-minute log-returns at day $t-j$. For the regressions we use daily data samples from 09/01/2007 to 08/31/2014. *,** and *** indicate statistical significance at the 90, 95, and 99% confidence level. The t-statistics are stated in parentheses.

Restricted Regressions for Daily VIX Straddle Excess Returns with Maturity of Four Months								
	(1)	(2)	(3)	(4)	(5)	(6)	(7)	(8)
Intercept	-0.0085^{**}	0.0000	-0.0002	-0.0038^{**}	0.0021^{**}	0.0021	0.0000	0.0012
	(-1.9781)	(0.034)	(-0.2613)	(-2.4469)	(2.5768)	(0.4216)	(-0.0779)	(0.2374)
$\text{VVIX}^{30\text{D}}$	0.0013^{**}					-0.0003		0.0000
	(1.9796)					(-0.4207)		(-0.0088)
$\text{Slope}^{\text{VVIX}}$		0.0031^{***}				0.0032^{***}	0.0029^{***}	0.0031^{***}
		(4.7219)				(4.2993)	(4.3479)	(3.8622)
$\text{Slope}^{\text{VIX}}$			-0.002^{***}				-0.0016^{**}	-0.0017^{**}
			(-2.9659)				(-2.3347)	(-2.3786)
$\text{VIX}^{30\text{D}}$				0.0019^{***}				-0.0006
				(2.6155)				(-0.6023)
VRP					-0.0031^{***}			
					(-4.1871)			
$\text{r}_t^{\text{Straddle}}$	0.0011	0.0005	0.0011^{*}	0.0011^{*}	0.0021^{***}	0.0005	0.0002	0.0003
	(1.5985)	(0.7243)	(1.7514)	(1.7029)	(3.2693)	(0.7911)	(0.3751)	(0.3805)
adj. R^2	0.0062	0.0207	0.0101	0.0085	0.0170	0.0201	0.0243	0.0230

Table O.12: Rolling regression: $\text{r}_{t+1}^{\text{Straddle}} = \alpha + \beta_1 X_t + \beta_2 \text{r}_t^{\text{Straddle}} + \epsilon_t$, where $\text{r}_{t+1}^{\text{Straddle}}$ is the is the daily return of a straddle on the VIX with a maturity of four months from end of day t to end of day $t+1$. X_t is a vector of explanatory variables observed at the end of day t. VVIX is the implied volatility-of-volatility index, $\text{Slope}^{\text{VVIX}}$ is the second PCA component of the VVIX term structure, VIX is CBOE's volatility index, $\text{Slope}^{\text{VVX}}$ is the second PCA component of the VIX term structure and the variance risk premium (VRP) is calculated as the differential of the risk-neutral and the physical expectation of the variation of the stock index over the next 30 days. We define $\text{VRP}_t \equiv \mathbb{E}_t^{\mathbb{Q}} \int_0^{30\text{D}} (d \ln S_{t+u})^2 du - \mathbb{E}_t^{\mathbb{P}} \int_0^{30\text{D}} (d \ln S_{t+u})^2 du = \text{VIX}_t - \text{RV}_t$, where $\text{RV}_t = \sum_{j=1}^{21} \sum_i (r_{t-j,i})^2$ and $r_{t-j,i}$ are the ith five-minute log-returns at day $t-j$. For the regressions we use daily data samples from 09/01/2007 to 08/31/2014. *,** and *** indicate statistical significance at the 90, 95, and 99% confidence level. The t-statistics are stated in parentheses.

Restricted Regressions for Daily VIX Straddle Excess Returns with Maturity of Five Months								
	(1)	(2)	(3)	(4)	(5)	(6)	(7)	(8)
Intercept	-0.0075^{*}	-0.0005	-0.0007	-0.0030^{*}	0.0007	0.0018	-0.0005	0.0025
	(-1.7595)	(-0.8687)	(-1.1398)	(-1.7536)	(0.7616)	(0.3534)	(-0.8866)	(0.4556)
VVIX^{30D}	0.0010					-0.0003		-0.0001
	(1.6166)					(-0.4629)		(-0.1216)
$\text{Slope}^{\text{VVIX}}$		0.0024^{***}				0.0026^{***}	0.0024^{***}	0.0030^{***}
		(3.7191)				(3.3755)	(3.6478)	(3.2817)
$\text{Slope}^{\text{VIX}}$			-0.0009				-0.0004	-0.0001
			(-0.7851)				(-0.3341)	(-0.1208)
VIX^{30D}				0.0013				-0.0013
				(1.4563)				(-1.0849)
VRP					-0.0021^{*}			
					(-1.9601)			
$\text{r}_t^{\text{Straddle}}$	0.0000	-0.0004	0.0002	0.0001	0.0008	-0.0004	-0.0005	-0.0004
	(-0.0473)	(-0.7031)	(0.4076)	(0.1400)	(1.2348)	(-0.5999)	(-0.7346)	(-0.6012)
adj. R^2	0.0009	0.0121	-0.0011	0.0004	0.0021	0.0113	0.0112	0.0105

Table O.13: Rolling regression: $\text{r}_{t+1}^{\text{Straddle}} = \alpha + \beta_1 X_t + \beta_2 \text{r}_t^{\text{Straddle}} + \epsilon_t$, where $\text{r}_{t+1}^{\text{Straddle}}$ is the is the daily return of a straddle on the VIX with a maturity of five months from end of day t to end of day $t+1$. X_t is a vector of explanatory variables observed at the end of day t. VVIX is the implied volatility-of-volatility index, $\text{Slope}^{\text{VVIX}}$ is the second PCA component of the VVIX term structure, VIX is CBOE's volatility index, $\text{Slope}^{\text{VVX}}$ is the second PCA component of the VIX term structure and the variance risk premium (VRP) is calculated as the differential of the risk-neutral and the physical expectation of the variation of the stock index over the next 30 days. We define $\text{VRP}_t \equiv \mathbb{E}_t^{\mathbb{Q}} \int_0^{30\text{D}} (d \ln S_{t+u})^2 du - \mathbb{E}_t^{\mathbb{P}} \int_0^{30\text{D}} (d \ln S_{t+u})^2 du = \text{VIX}_t - \text{RV}_t$, where $\text{RV}_t = \sum_{j=1}^{21} \sum_i (r_{t-j,i})^2$ and $r_{t-j,i}$ are the ith five-minute log-returns at day $t-j$. For the regressions we use daily data samples from 09/01/2007 to 08/31/2014. *,** and *** indicate statistical significance at the 90, 95, and 99% confidence level. The t-statistics are stated in parentheses.

O.2 Additional Figures

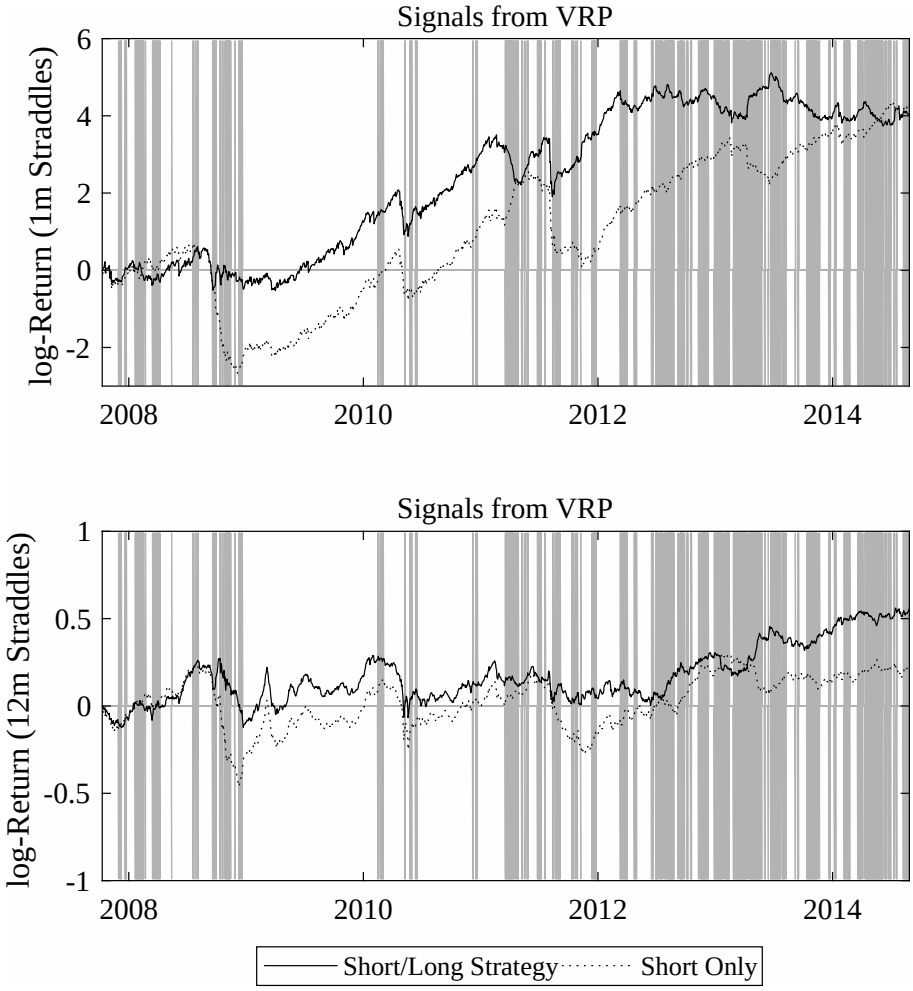

Figure O.1: The figure shows logarithms of return paths for different S&P500 constant maturity straddle strategies. The panels show strategies which use a signal from the VRP. In the top panels we plot strategies for one month straddles and in the bottom panel we plot strategies for twelve month straddles. The baseline strategy is going short in the straddles. If the VRP is in the lowest historic 75% quantile on day t, the strategy goes long straddles, which is marked by grey areas. The portfolios are adjusted on a daily basis and the quantile is calculated using only information until day t. The burn-in phase is one month (September '07) and trading costs are omitted.

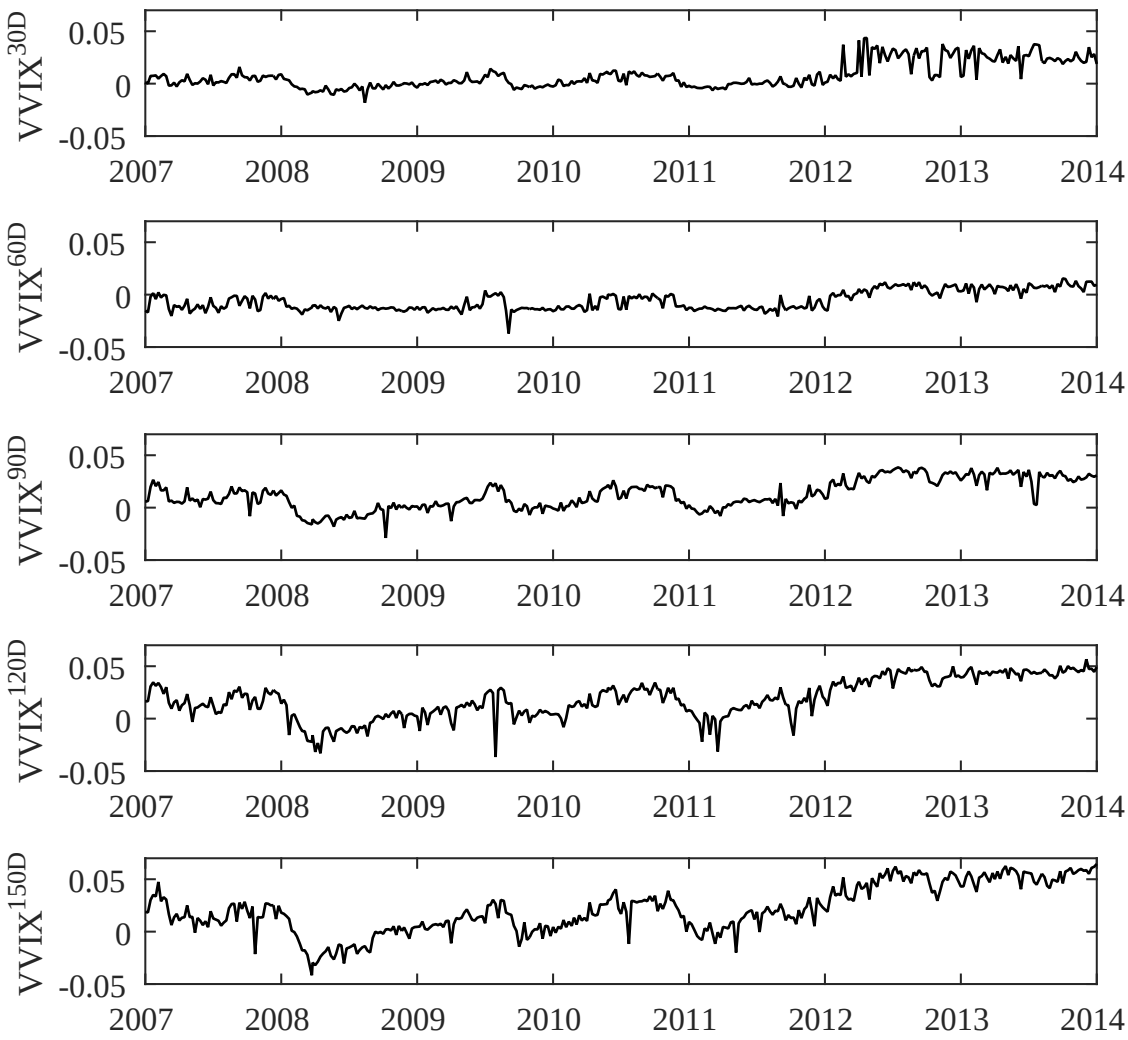

Figure O.2: The figure displays the relative errors $\epsilon_t^{\text{VVIX}^\tau} \equiv \frac{\sqrt{A^{\text{VVIX}}(\Theta,\tau)+B^{\text{VVIX}}(\Theta,\tau)'\widehat{Y}_t}}{\text{VVIX}_t^\tau} - 1$ of the VVIX approximation for the maturities $\tau = 1, 2, 3, 4, 5$ months.